GLACIER CHANGE AND BEHAVIOUR: HAZARDOUSLY ERRATIC, CLIMATICALLY REGULAR

EASTERN CENTRAL CAUCASUS MOUNTAINS, RUSSIA, 1971 – 1999

SCOTT POLAR RESEARCH INSTITUTE
UNIVERSITY OF CAMBRIDGE

Tiffany Lee Lunday
M.Phil. Dissertation
8th June 2007

ACKNOWLEDGEMENTS

The experience of producing this work was in many ways, a long and lonely journey of exploration and discovery. There were many times when the work was too difficult or the task seemingly insurmountable. During this task, there were some people who made the journey ever more bearable and even enjoyable. I want to take the opportunity now to thank them.

The staff at the Scott Polar Research Institute have been ever helpful and patient with this new student along the path to completion. Thank you. My family and friends have been ever supportive; especially my mom and Dave, who always have a free ear, welcome advice and lots of encouragement.

And finally, to my supervisor, Gareth Rees, without whose constant guidance (and sometimes intervention) none of this work would have been possible. He has been a great teacher when I've needed it and a great friend when I needed that too. Thank you.

Tiffany Lunday

June 8th, 2007

CONTENTS

CHAPTER 1

INTRODUCTION

Glaciers, excluding those of the Antarctic and Greenland icesheets, comprise about 4% of the total land ice of the earth, and, melted, would only contribute a total of 0.5 metres water equivalent (mwe) to sea-level rise (Dyurgerov, 2002; Warrick et al, 1996). However, rapid melting over the last century has ensured that perhaps as much as 30% of the total contribution of melting ice to the rise in sea level during the same period (Meier 1984). The most frequently cited mechanism explaining this phenomenon is an overall warming global climate (Warrick et al, 1996). Many of these glaciers are concentrated in regions where population densities are high, as in the Alps and the Caucasus. But even where population densities are not high, small glaciers are a local source of freshwater, significant for both the natural and anthropogenic environment (Fagre et al. 1997 *in* Hall and Fagre, 2003; Oerlemans et al. 1998). Not only does their growth and decay have a profound effect on their local and regional surroundings, they are a major indicator of climate changes and fluctuations (Dyurgerov, 2002). It is these facts and figures that justify the close and careful scrutiny of small glaciers now and in the future.

In terms of worldwide glaciological research, there is a bias in data for the Alps, where the longest, most complete and numerous time series are available. Roughly 70% of all existing mass balance measurements are from Europe, the USA, Canada and Russia (Dyurgerov, 2002). Glacier inventories are lacking for many areas as well, especially with respect to glacier class size and distribution (Oerlemans, 1998).

The Caucasus region of Russia has had a decreasing influx of glaciological data as a result of program cancellations and economic concerns (Dyurgerov, 2002). This is true not only for mass balance programs, but also for other glacier and climate studies (e.g. high-altitude climate studies). There are only two glaciers in the Caucasus with adequate mass balance time series, Djankuat and Gergeti Glaciers, despite the fact that the region has relatively easy field access. Neither of the two glaciers falls within the area of this study. For the tens of glaciers within easy field access in the Eastern Central Caucasus, not one has mass balance measurements. However, it appears that the present and recent political climate has not fostered an environment conducive to field research (Rees, W.G. pers. comm.).

Of the data available for the Caucasus Mountains, the vast majority of it is non-English (i.e. Russian and Georgian) literature (e.g Katalog Lednikov). This means that a great deal of information is inaccessible to the community of English-speaking researchers. There is also an issue about nomenclature for glaciers in the Caucasus, because the region straddles the Russia – Georgia border and the names of glaciers and geographical features are not always consistent. The lack of glacier measurements in that region, coupled with the fact that much of the information that would be available for study is not in English makes it a good candidate for glaciological research.

1.1 GLACIERS AND CLIMATE CHANGE

Glacier response to climate change has long been established as a fundamental truth about glacier behaviour. For nearly half a century, it has been recognized that the glacier mass balance is the crucial link between climate and glaciers (Meier 1965). This link highlights the mutual relationship between glacier and climate studies; climate change is predictive of glacier behaviour, while glacier behaviour is an indicator of the changing climate. Glaciers have even been quoted as "sensitive climatological stations, collecting data... in widespread and remote locations over great spans of time." (Harper, 1993) In particular, mountain and valley glaciers are very useful indicators of climate change due to their relatively fast, regular response time to fluctuations in climate (Oerlemans 2002). The overall result has been that glacier studies, and mass balance studies in particular, have received increased attention in terms of climate change (Meier, 1984; Oerlemans and Fortuin, 1992; Kuhn, 1993; Dyurgerov and Meier, 1997).

The glacier mass balance describes the net gain or loss of snow and ice over a given year, termed the 'mass balance year,' typically measured from the start of the accumulation season to the end of the melt season (Benn and Evans, 1998). Mass balance and glacier volume measurements are systematic investigations of changes in glacier ice volume, and it has been shown that these balance changes (i.e. ice volume changes) eventually manifest themselves in terms of glacier morphology and behaviour (Oerlemans, 2002).

These include, among other characteristics: glacier size, shape and terminus location. Because the behaviour of these characteristics is normally dependent on and a reflection of the mass balance regime of a glacier, there is support for the idea that these properties, too, are invaluable for glacier - climate research.

Although mass balance studies are the main vehicle through which the glacier - climate relationship is most effectively analysed (Meier, 1965), mass balance records are not always available, and for many regions are severely lacking or absent (Dyurgerov, 2002). The lack of mass balance measurements are a reflection of the inaccessibility of some glacier regions and the high cost of performing field studies (Harper, 1993). It has been widely recognized that other channels for studying glacier behaviour are necessary to adequately describe worldwide glacier fluctuations (Harper 1993). The World Glacier Monitoring Service (WGMS) has published seven volumes of Fluctuations of Glaciers (FoG), which include terminus position measurements in addition to mass balance records for hundreds of glaciers around the world (FoG 1967, 1973, 1977, 1985, 1988, 1993, 1998).

Estimations of the shape and extent of glacier ice coverage have been attempted from early on in glacier studies (see Field, 1975 for the Caucasus). Because mass balance refers to gains and losses of snow and ice (i.e. volume measurements), the overall extent of glacier ice is directly affected by changes in mass balance[1]. Therefore studies involving assessment of glacial coverage are, in effect, describing the mass balance regime to a considerable extent. This type of data goes back further than systematic investigations of mass balance, and is available for a wider number of regions and glaciers (WGMS website, 2007). Glacier size and shape is not only useful as an indication of the mass balance regime, but it also sheds light on the interaction of the glacier with its immediate environment (i.e. how slope and aspect may affect differential melting or how local orographic effects may exercise control).

The glacier terminus position describes one aspect of glacier size and shape. It is a widely used marker for glacier – climate studies when mass balance data is not available, and is

1. This is also true for ice thickness, although in areal studies like this one, thickness is not considered.

supplementary information when it is. The relationship between mass balance and terminus positions is obvious; during times when the balance is primarily negative, the glacier terminus typically migrates up-valley. There are exceptions to this rule, which depend on the internal dynamics of the individual glacier. The WGMS glacier internet database provides a clue to how much more widely available terminus position measurements are compared with mass balance measurements. And in modern times, remote sensing has opened up a new channel through which we can effectively go back in time to supplement, verify or replace existing measurements for glacier termini.

1.2 PHYSIOGRAPHIC CONTEXT

Before embarking on a study of Caucasus glacier behaviour, it is important develop a physiographic context. We have emphasized the effect of climate on glacier behaviour; however, climate is not the sole determinant. This is especially the case for the Caucasus region, where glaciers exhibit a strong response to other physiographic elements such as topography and orography. The question of how these glaciers have physically evolved in terms of shape and size is only answered when a full knowledge of the area and the forces acting in it has been achieved. Moreover, we will see later that these forces assist in explaining some of the observed characteristics of some of the glaciers.

Climate obviously exerts a major influence, affecting the glacier mass balance regime. At the macro-, meso- and microscale, climate has a profound affect on glacier regime, which in turn feeds back to affect local climate (Oerlemans, 2002). The physical characteristics of the environment also play a major role, including slope and aspect of the mountain range. Geologic and tectonic forces control much of the actual physical and thermodynamic regime of the glaciers, which leads to specific internal stress and deformation characteristics that contribute to the way they move. How and to what extent these factors influence observed glacier behaviour is debatable[2], but they all interplay to ultimately determine the evolution of Caucasus glaciers.

1.2.1 CLIMATE

This study focuses on the glaciers of the eastern-central portion of the Greater Caucasus Range (Figure 1.0). Altitudes here range from roughly 2,500 in the mountain passes to peaks over 4,000m. The highest peak in the study is Mt. Kazbek at 5,034m.

The range spans the distance between the Black and Caspian Seas. The high elevations produce well-developed, vertical climatic zones (Lydolf 1977). In the highest reaches of the mountains, the climate is very cold and precipitous, ideal for sustaining glaciers.

As a horizontal barrier, the mountains tend to be most effective in winter, when air masses are not more than 2,000m thick. However, summer air masses are 6,000m or more and can cross the range (Lydolf 1977). This characteristic contributes significantly to the north – south distribution of glaciers. The atmospheric circulation over the Caucasus is dominated by a zone of suptropical high pressure in summer and the Asiatic high in winter (Lydolf 1977). In winter, when the northern flanks of the mountains are influenced by the Asiatic high, the southern side remains relatively warmer, as the influence comes from the subtropical system in the south. In summer, temperatures are more evenly distributed across the range. There is some evidence that very distant modes of atmospheric circulation may also significantly impact regional climatic conditions in the Caucasus. Teleconnection patterns originating at the ocean-atmosphere interface in the tropics show some correlation with climate variables in the Caucasus (Shahgedanova 2005).

The overall mountain climate tends to have low-amplitude annual temperature changes, particularly compared with the surrounding climatic zones. The temperature remains below zero for most of the year. Even in summer, when air temperatures are normally above freezing, the temperature can drop below zero. In the very high mountains, blizzards and snowstorms are common and may contribute significantly to the winter accumulation. Conversely, there are sometimes spring temperature inversions that result

2. There has long been discussion and speculation as to the actual causes of major glacier events such as glacier hazards and failures, which still remain largely unknown (see Tutubalina, 2006).

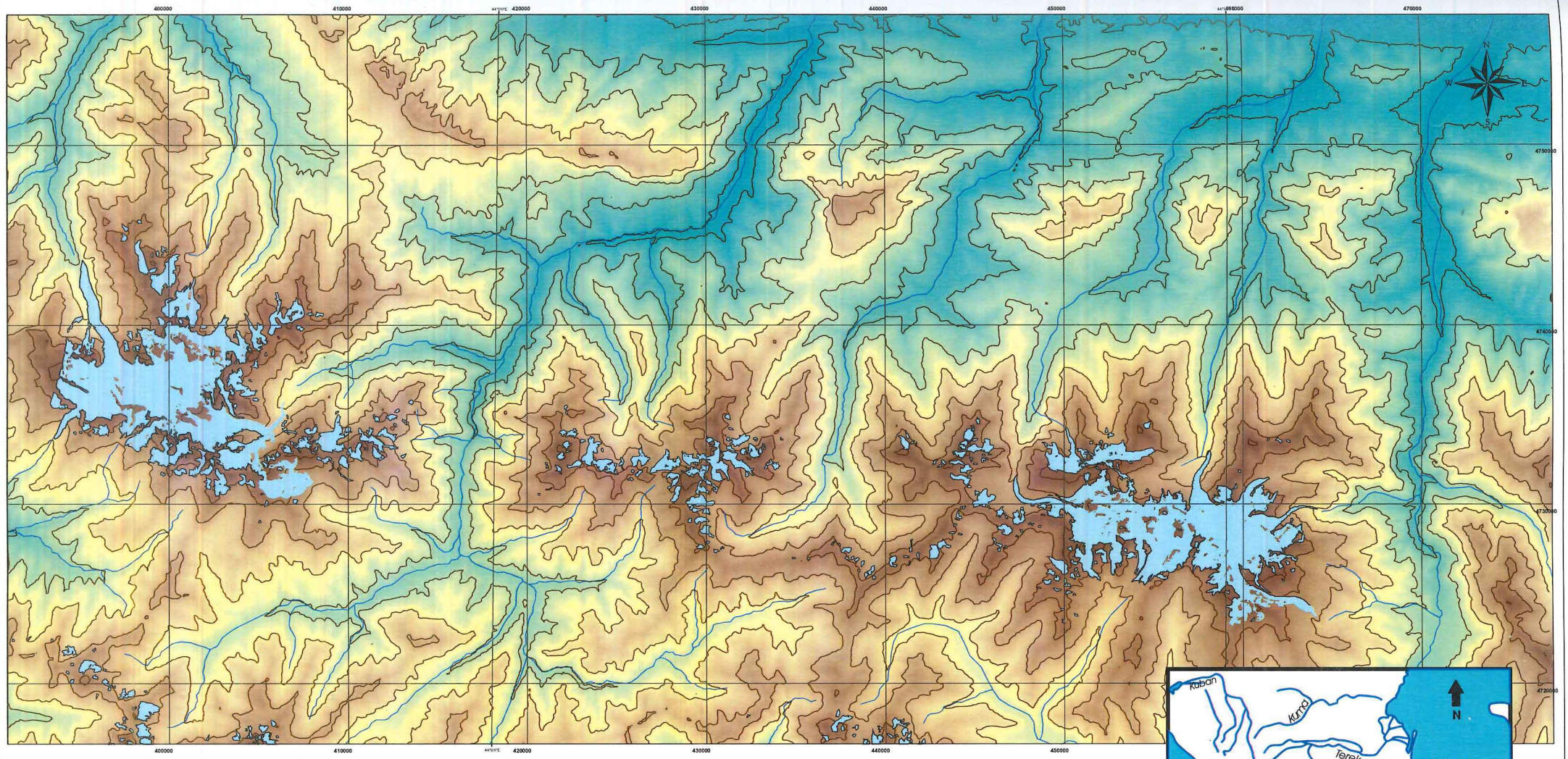

Figure 1.0: Regional Map of the Study Area

in high temperatures at high altitudes and may cause avalanching (Lydolf 1977). In fact, avalanching is common in some parts of the Caucasus. So common on some glaciers in the Caucasus that it can be a major source of accumulation.

1.2.2 Glacier Classification and Regime

For decades, researchers have preferred a climatic classification of glaciers based on the predominance of individual mass balance characteristics (Schytt 1967; Kuhn 1979, 1984). Glacier regime is defined as a result of in-situ measurements carried out on glaciers worldwide (Dyurgerov, 2002). General divisions include polar/subpolar, maritime and alpine/continental (Kuhn, 1984). Maritime glaciers have much higher levels of both accumulation and ablation than continental glaciers, resulting in a higher mass turnover. Their existence is generally sustained by high levels of winter snowfall, while in the summer months very warm temperatures deplete them. High glacier mass turnover generally means that a glacier will respond more quickly to climate change (Oerlemans, 1993). However, it also produces measurable responses to short-term fluctuations, or noise, in the overall climate signal (Oerlemans, 2002).

The Central Greater Caucasus had traditionally been categorized as having relatively dry, continental-type glaciers because of their continental location (Horvath and Field, 1975). This perception has changed, however, with analysis of actual climate and mass balance data. The glaciers are located at high altitudes in a subtropical setting, flanked on the west and east by the Black and Caspian seas. The melt season is considerable (May – Sept) and precipitation levels are high due to the proximity of the Black Sea, which produces a very maritime-type climate (Lydolf, 1977). The Black Sea is the major provider of moisture to the region, with precipitation increasing sharply westward, reaching very high regional levels in the area of this study. Precipitation provided to the glaciers can be great. It is generally concentrated in the summer months, when the temperatures are usually above zero. However, their high altitude often ensures low summer temperatures. If summer temperatures drop below zero, precipitation falls in the form of snow. In the winter, the temperature almost always remains below freezing, causing all precipitation

to fall as snow. The combination of summer temperature and precipitation jointly regulate the glacial regime, which tends between maritime and continental conditions. In assessing glacier behaviour, I will approach it from that angle.

Because the Caucasus region tends between the maritime and continental extremes, mass turnover is relatively high, producing quick responses to the overall climate trend. At the same time, annual and short-term fluctuations are muted with respect to the prevailing climate signal. This is probably mostly because of the even effects of summer and winter climate on mass balances. The overall mass balance regime of Caucasus glaciers appears to be jointly regulated by wintertime levels of precipitation and summertime temperatures. Accumulation and ablation data statistics for Djankuat Glacier support this idea (Shahgedenova 2005).

1.2.3 AVALANCHING

A few Caucasus glaciers rely on avalanches for a significant part of their nourishment throughout the year (Perov, 1978). Avalanching is actually more significant on Mt. Elbrus in the west than it is near Mt. Kazbek. Alhough there is no single glacier in this study area that is fed solely by avalanching, it is still important to recognize that it contributes to the redistribution of snow. The structure of the mountains coupled with the climate is the mechanism for avalanching. A good example of an avalanche-fed glacier is the Donguz-Orun Glacier immediately to the south of the south flanks of Mt. Elbrus (Figure 1.1). It is fed primarily by avalanching and the Semerka Glacier to the north. Similar to many glaciers in the study area to the east, it is heavily moraine covered and presents the challenging task of synthesizing the various forces acting on it to form an explanation of its evolution.

Figure 1.1 Donguz-Orun Glacier, southern flanks, Mt. Elbrus. Note the debris-covered ablation zone in the foreground, and avalanching from the steep slopes. This glacier typifies the glacial physiography of the Caucasus Mountains.

1.2.4 High Mountain Hazards and Debris Cover

As a tectonically unstable region, the Caucasus is prone to a wide variety of hazards and mass wasting events (Huggel et al., 2006; Tutubalina, 2007). These events are largely the result of tectonic instability and geological structure (Huggel et al., 2006) and can be either very minor or catastrophic. As a result, it is typical for the glaciers to have a lot of debris cover, due to the fact that they experience exceptional mass wasting in the form of rock falls and debris flows. Debris at the glacier surface can often help lead to more catastrophic events in which the glacier may detach from parts of its bed and become entrained with the downward movement of other debris. Though they were identified in literature decades ago (Heybrock, 1935) (albeit with confusing nomenclature), these events have been re-termed 'glacier disasters' (Tutubalina, 2007) and profoundly affect glacial regime.

High mountain hazards are a potential and ongoing threat in the Caucasus, and as a result, the Caucasus received a great deal of attention during the 2004 International Conference on High Mountain Hazards. Hazards are so common in this area, particularly in the east around Mt. Kazbek, that much of the contemporary research and literature is focussed on these events (e.g. in Proceedings of the International Conference on High Mountain Hazard Prevention, Vladikavkaz-Moscow, 2004), while glacier-climate studies are apparently significantly fewer in number.

Glacier headwalls are typically steep, with rock cleavages oriented in plane with slope surfaces (Huggel et al. 2005). Work with a DEM for the area shows very steep slopes indeed - especially at high elevations (Figure 1.2). The general trend is a shallowing out near the ablation zone where there grades are smaller. Debris falls from all angles to land at the glacier surface, often obscuring much of or even the entire glacier. The steep head- and sidewalls immediately adjacent to glaciers provide the mechanism by which large amounts of snow can become buried. In remote sensing studies, determining the absolute extent of glaciers is severely hindered by accumulation of surface debris.

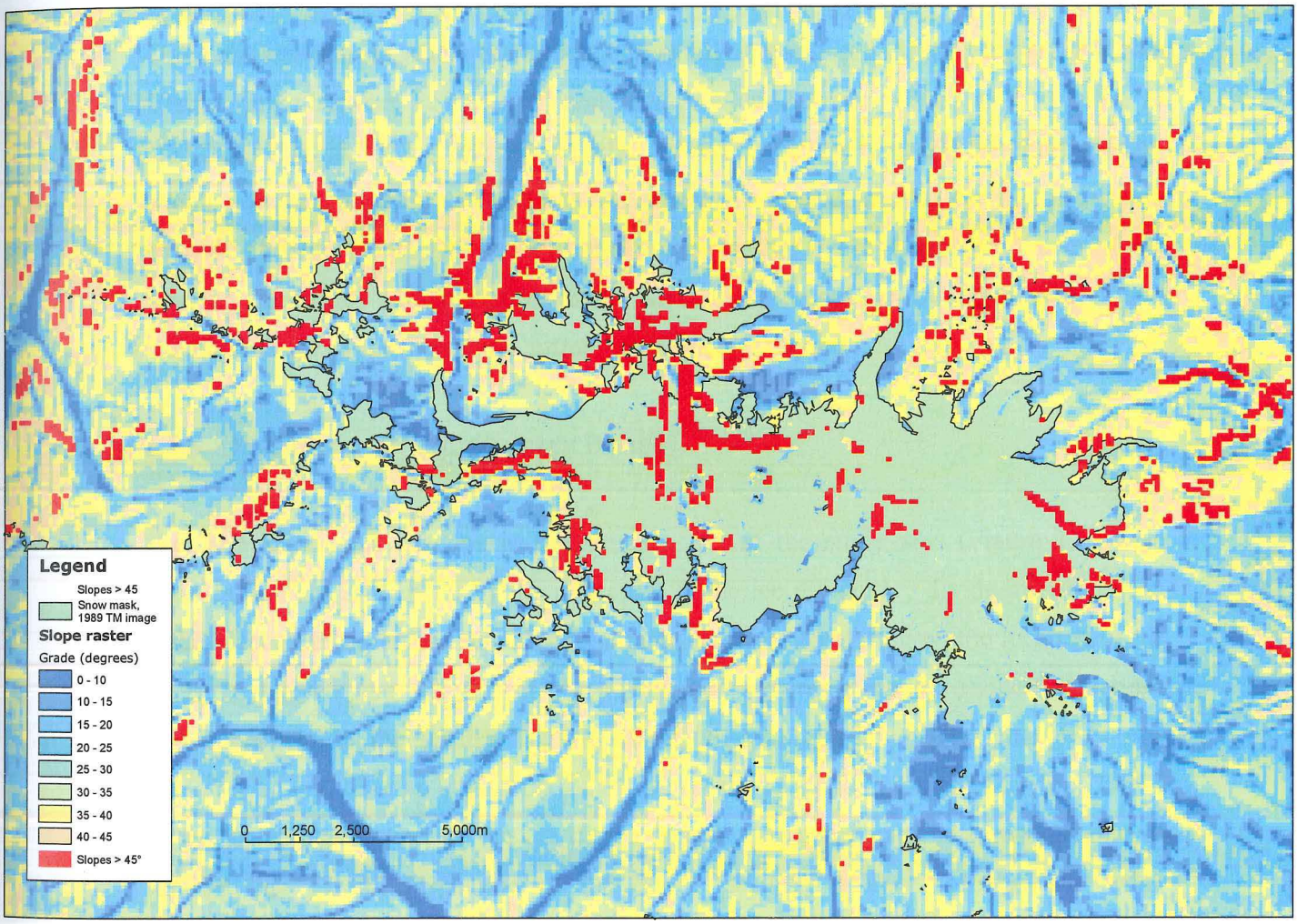

Figure 1.2 Slope Analysis, Mt. Kazbek Region

The problem with debris cover in remote sensing analyses appears repeatedly throughout literature and analyses (Paul et al., 2003). It remains likewise problematic in the Caucasus area, where it is exaggerated by the fact that the Eastern Central Caucasus has a small glaciated area, so that the proportion of debris-covered ice to clean ice is relatively high.

There are a few areas where the effect is especially pronounced. Slopes above the Kolka Glacier range between 45° and 70° and have provided so much debris to the surface of the glacier that, in 2002, a massive landslide forced the failure of nearly the entire glacier, which became entrained in the mass movement (Huggel et al., 2006). Historical data shows that these events are not unusual (Tutubalina, 2007). On the eastern flanks of Mt. Kazbek, landslides and glacier disasters have also occured on Devdorak and Abano Glaciers. These events massively influence the glacier regime.

1.2.5 Migration of the Glacier Divide

Tsei and Karaugom Glaciers in the western part of the study area (Figure 1.3) have regimes that are influenced by the migration of the ice divide. Ice divide migration can make glaciers more or less sensitive to climate changes, depending on the location of the divide in a given year. The parcel of ice contained within the area of divide fluctuations will contribute to the balance regime of one of two glaciers, and a change in this contribution will have an impact on the balance regime (Waddington and Marriott, 1986). Using an approximation of the ice divide is not correct for balance measurements. It follows that careful inspection of the divide position is also necessary for other measurements of glacier behaviour, such as glacier extent.

1.3 Remotely Sensed Imagery and Glacier Studies

The use of remotely sensed data in glaciological studies has gained increasing attention over the decades for glacier monitoring (e.g Bolsch, 2005) and glacier inventory (e.g. Paul, 2002). Its usefulness and practical application are now widely recognized. Early studies employed the use of airborne photographic techniques (Williams and Hall 1993),

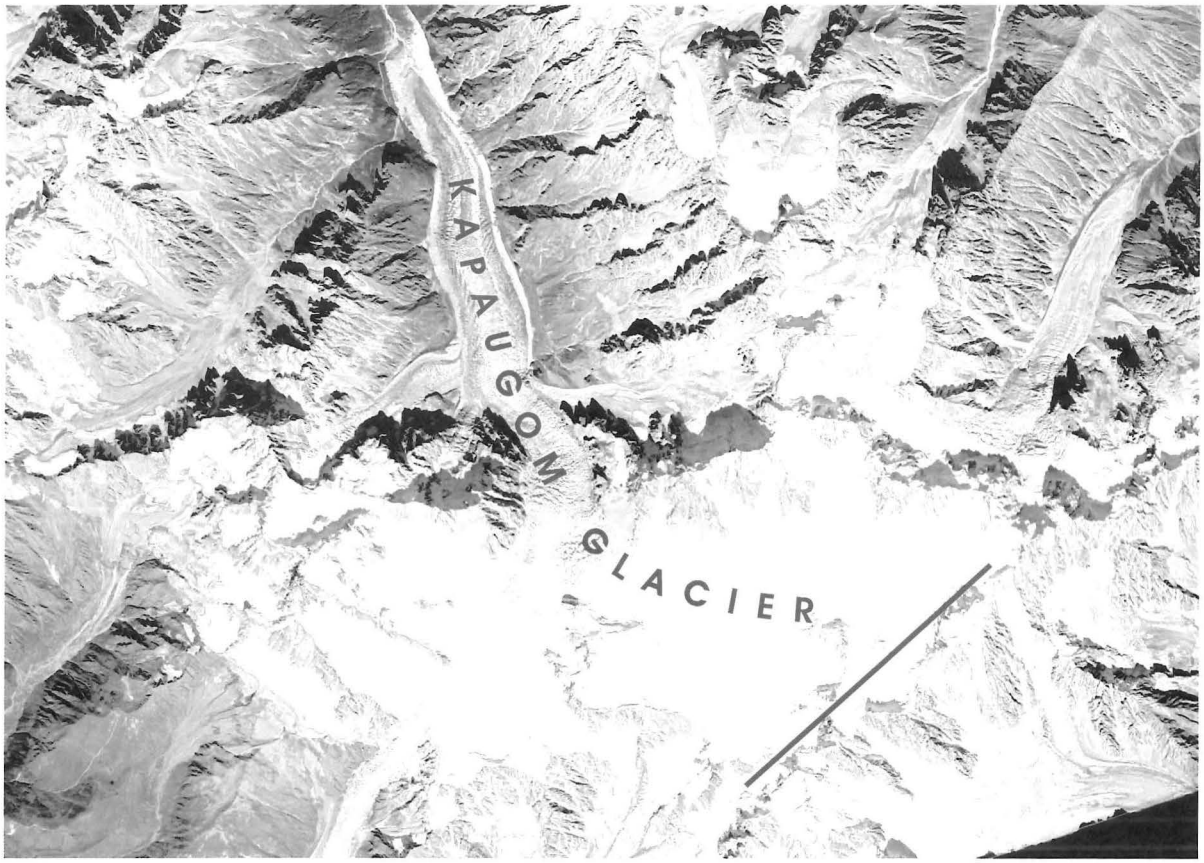

Figure 1.3 Kapaugom and Tseya Glaciers. The red line indicates the location of the ice divide

though the field has opened up over time with the application of spaceborne and digital techniques (Rees, 2006).

The application of remote data is a logical approach to glaciological studies, because glaciers and ice sheets are naturally located in regions with limited accessibility. Historical evaluations of snowcover and glacier extent were dubious simply because of the logistical impracticality of measuring vast areas of snow and ice. With airphotos, these measurements can be known to within only square metres of the actual values. And with digital methods (from sensor systems such as Landsat, ASTER, IKONOS, and the AVHRR), the temporal resolution is vastly improved from a lag time of years or decades between measurements to within weeks. The practicality of remote sensing lends easily to glacier-extent studies and today glacier inventories for most glaciated areas worldwide are either underway, completed, or in their second phase of coverage (e.g. the Swiss Glacier Inventory 2000 (Paul 2002), and the Patagonia Icefield (Aniya et al. 1996)).

There is invariably a trade-off between spatial and temporal resolution with the instruments in current operation. While airphotos still provide the best spatial resolution of any method (though this is very quickly changing), the radiometric and temporal resolution of such images is lacking. Spatial coverage is also often an issue, although the availability of hundreds of thousands of spy satellite photographs from the US government provides coverage of most of the globe. The Landsat devices have excellent radiometric and temporal resolution, although the spatial resolution for early images is only 89m by 69m.

With high spatial resolution, there is the possibility of resolving individual glacier features such as crevassing, moraines, debris, meltwater and termini (Rees, 2006). With time-series images, change detection is possible. The ability to view multiple dates of coverage and monitor glacial features is a widely-applied (Rees, 2006) and invaluable way of monitoring glacier behaviour over time.

Numerous types of data can be gathered with remote instruments. Beyond the familiar visible and infrared imagery created by photographic and visible and infrared (VIR) instruments, there are techniques that can be employed to measure surface topography, ice thickness (Nitikin et al., 2005 for surging Caucasus glaciers), ice temperature and snow facies (Hall et al., 1987; Orheim and Luccitta, 1987).

The Eastern Central Caucasus region has little known research that has been conducted with the use of remotely sensed imagery. However, coverage of the area by many commercial instruments is highly accessible and available. Therefore, in order to gain a greater understanding of glacier behaviour in the region, I consider that an attempt to construct a comprehensive picture through satellite imagery in the Eastern Central Caucasus is relevant.

1.3.1 CORONA Imagery

The earliest images available for this study were CORONA satellite photographs. The CORONA satellite was the first generation of the US reconnaissance satellites built by the US Air Force and Central Intelligence Agency (CIA) (Altmaier and Kany 2002). Taken between 1959 and 1972, these images represent the first-ever large-area coverage, high resolution satellite images (USGS 2007). The images were taken with a panoramic camera at a variety of scales ranging (6-460ft) on panchromatic film. For this study, images from the KH-4B flight mission were obtained. These images were flown at a nominal height of 150km, and have the best ground resolution at a mere 6ft. The mission used two cameras for forward and aft viewing, both positioned at 15deg to normal (30deg between them) in order to produce stereopairs (Figure 1.4).

The catalogue is large at over 880,000 images, released to the public by the Clinton administration in 1996 with an additional 50,000 released in 2000 (USGS 2007). Though the images have excellent ground resolution and good historical coverage, cloud cover is common. Much of the total area covered by the 930,000 images is obscured (USGS 2007). It is normal for this effect to be exaggerated at far north and south latitudes and in

mountainous regions. However, the primary motive for the satellite missions was to spy on the former USSR, so coverage tends to be biased toward Eastern Europe and Asia (Altmaier and Kany, 2002). Therefore, coverage over the Caucasus Mountains is relatively good, and fortunately, the acquired images are nearly completely cloud-free.

The images used for this study, as mentioned, are from the last and highly successful KH-4B mission. The flight direction was south-southeast – north northwestwards, with forward and aft images having nearly perfect overlap. Images were scanned at a resolution of 21 Micron (1200 dpi), resulting in a realized ground resolution of approximately 10ft.

The CORONA images are as yet a relatively underused source of high-resolution landcover information, though some studies have tried employing them (Altmaier and Kany 2002). This may be due to the difficulty of using the images; they have varying scales, large files, lots of cloud cover and variable temporal resolution. They are by no measure systematic.

1.3.2 LANDSAT IMAGERY

Ground Coverage

The Landsat satellites have provided uninterrupted coverage of the earth since 1972. All of the sensors have been line scanning devices observing the Earth perpendicular to the orbital track; the cross-track scans are accomplished by an oscillating mirror. The scanners are in polar, sun-synchronous orbit, and image during the descending (north to south) orbital path.

Images are inventoried by the World Reference System (WRS) in which all scenes are identified by a unique path and row (CEOS website, accessed Dec. 2006). Currently, a Landsat satellite returns to its WRS point of origin and repeats the cycle every 16 days. Combined coverage by Landsats 5 and 7 provided repeat imaging every 8 days for all

locations covered by the WRS (until a mechanical failure of Landsat 7 in May 2003 which has caused data gaps since then). At the equator, the ground track separation is 172 km, with a 7.6 percent overlap at scene edges. This overlap gradually increases as the satellites approach the poles, reaching 54 percent at 60° latitude. This fact is advantageous for polar and northern studies, as ground coverage will be greater in those regions.

Four types of sensors have been employed since the start of the Landsat missions. Three of them provided images used in my research. Technical specifications for those three are described in detail below.

Multispectral Scanner (MSS)

The multispectral scanner was the first scanning device to provide high-resolution, multispectral images of the earth's surface. Landsats 1 through 5 carried the MSS sensor. The carriage of an MSS sensor onboard Landsats 4 and 5 (which also carried the improved Thermal Mapper) was intended for data continuity in landcover studies. It was later dropped from Landsats 6 (which failed before orbit) and 7. The spectral coverage was obtained over four band wavelengths, ranging from green to near-infrared (near-IR). Landsat 3 carried an MSS sensor with an additional thermal infrared (thermal-IR) band, designated band 8.

An MSS scene had an Instantaneous Field Of View (IFOV) of 68 meters in the cross-track direction and 83 meters in the along-track direction. Images are resampled and provided for use at a ground resolution of 57m.

Thematic Mapper (TM)

The Thematic Mapper (TM) is an improved multispectral scanning sensor with higher image resolution, sharper spectral separation, improved geometric fidelity and greater radiometric accuracy and resolution than the MSS sensor. The first six years of operation

of the MSS provided an opportunity to identify places where the sensor could be made more useful for environmental monitoring. The Thermal Mapper has seven spepctral channels. The thermal-IR imaging capabilities of the TM are improved over the MSS with a ground resolution of 120m. The other six bands are imaged with an IFOV of 30m and ground resolution of 27.5m.

Enhanced Thematic Mapper Plus (ETM+)

The earth observing instrument onboard Landsat 7, the Enhanced Thematic Mapper Plus (ETM+), replicated and improved upon the capabilities of the Thematic Mapper instruments on Landsats 4 and 5 until a mechanical failure in May 2003. Since then there have been gaps in image acquisition. The main improvements over the TM sensor were a ground resolution of 60m in the thermal-IR channel and an additional 15m ground resolution panchromatic channel.

The purpose of this study is a description of glacier change during the years between 1971 and 1999. Altogether, that period is inclusive of 28 mass balance years. The time period is long enough to be able to resolve change between images with the ground footprint of all the images, including at the 57-metre resolution of the MSS data. The most significant comparison that will be made is between the 1971 Corona satellite images and the 1999 ETM+ images. Even so, other comparisons between images provide a better understanding of change over time. The Landsat images acquired at the intermediate dates are useful and timely, as they represent decadal changes during the 28-year period. The production and release by NASA of geodetic Landsat images for those time periods was designed for environmental change detection studies like this one (Tucker et al., 2004).

CHAPTER 2

METHODS

2.1 IMAGE ACQUISITION

The images were taken near the end of the ablation season to minimize the amount of potential snow cover and obtain a clear view of the glaciated area. Two types of satellite images were used: satellite photography and digital satellite images. All images used in the study were obtained from different sensors, representing different levels of technology and spanning a total of 28 years (see Table 2.1).

Satellite	Sensor	Acquisition Date	Ground Resolution	Image Type
CORONA	KH-4B (camera)	20-Sep-1971	6ft.	Photographic
Landsat	MSS	25-Aug-1978	57m	Digital
Landsat	TM	26-Sep-1987	28.5m	Digital
Landsat	TM	31-Aug-1989	28.5m	Digital
Landsat	ETM+	18-Aug-1999	30m	Digital

Table 2.1 Images used in this study and some of their technical specifications, including sensor name, acquisition date (the date on which the sensor took the image) and ground resolution

Landsat imagery is a digital form of data that is highly accessible and ready-to-use, thanks to the USGS and to programs like the one that produced the GeoCover dataset. It is intended for environmental monitoring and research. Because it is digital, it can be accessed very quickly. Conversely, CORONA imagery is in analog format and requires a very high degree of pre- and post-consumer image processing. The photographs come in scanned, digital format when they arrive, but do not have any radiometric, geometric or terrain corrections applied. Because of the pre-consumer scanning process, it takes a few weeks to obtain the images. Therefore, late arrival of the CORONA imagery from the USGS prompted use of the readily accessible Landsat images first. It was through those images that my initial, firsthand assessment of glacier distribution, morphology and behaviour was made.

The Landsat images earned a great deal more attention and time than the CORONA images for two reasons. The first, as mentioned, was a great delay in obtaining the CORONA data. Pressed for time, it was imperative that many different methods be

employed on the Landsat scenes in order to gain as much information as possible about glacier conditions. Secondly, because it was so difficult to analyse parts of the Landsat scenes due to the large amount of debris on the surface of glaciers, the process of actually getting that information about glacier behaviour was drawn out considerably.

For the CORONA images, basic air photo interpretation was the fastest and most useful method. The photos are stereopairs, and therefore stereoviewing was helpful. However, at a nominal resolution of 6ft, individual images without stereoviewing were sufficient to lead to a thorough firsthand knowledge of regional physiography and glacier terminus positions. The image ground resolution is remarkable. There were even cases where the detection of glaciers that would have gone completely unnoticed in the Landsat image was possible. Moreover, very small glaciers and patches of permanent snow were detected quite easily along with their total extent and terminus positions. This enabled study of very small glaciers, which is important for short-term climate analysis.

2.2 Image Compatibility

Environmental and land cover changes occur on the land surface on the order of metres to tens and sometimes hundreds of metres over time (Townsend and Justice, 1988; Townsend and Justice 1990). It follows that environmental monitoring projects require data at spatial resolutions on the order of tens of metres to adequately capture surface dynamics (Tucker et al., 2004). Landsat and CORONA missions are both capable of providing this resolution, contingent on whether or not within- and among-scene georegistration is achieved (Townsend et al., 2002).

Both the CORONA and the Landsat scenes suffered from problems associated image geometry and georeferencing. Through initial image processing it was found that the Landsat images, though nominally ready-to-use, needed to be normalized and made compatible with each other.

What is meant by data 'normalization' and 'compatibility', and what do they involve? By data normalization, I mean that all individual geographic data must be accurately georeferenced to a coordinate system. Compatibility refers to the need for georeferenced datasets to have accurate between- and among-date registration (also referred to here as geodetic compatibility). Without adequate, relative compatibility among images, detected changes and the interpretations that result from them are meaningless (Townsend et. al, 1992).

For glacier studies, these requirements have several implications. The above definitions explicitly state that the same coordinates and coordinate system must reference the same features in all datasets. Typically, this can be achieved by using a number tie points, or ground control points (GCPs) common to all images. Having the same projection system for all images is important in contemporary studies, though it is not nearly as difficult to achieve as it has been in the past thanks to current technology. Software packages use standard on-the-fly projections for all digital datasets (ERDAS Imagine, ESRI ArcGIS). Therefore, most data in digital form can easily be presented in a common projection.

Beyond the above requirements, for glacial studies it is necessary that there be good temporal agreement. It has been demonstrated that mass balance and climate studies have a strong seasonal influence. This seasonal influence is so extreme that glacier behaviour exhibits two phases during the year, a summer and a winter phase. Glacier studies are typically defined by this seasonal division; where summer and winter mass balances are measured separately and then recombined to yield a net annual balance[1]. The summer and winter seasons are so different in nature that air- and spaceborne imagery exhibit few similarities between seasons. Therefore, acquisition dates for the imagery need to agree within a narrow time frame. For the Caucasus there is a window of about a month where images show adequate temporal agreement during the end of the ablation season. And as noted above, all images were acquired neatly within this window.

For change detection studies in general, there should also be (though this is not entirely necessary) adequate agreement concerning the atmospheric conditions over the study

1. For very dry, continental glaciers a more appropriate division may be annual snow-ice accumulation (c_i) and annual ablation (a_i) (Dyurgerov, 2002; Oerlemans, 2002).

area. It is desirable to collect cloud-free data, and useful to have comparable ground and spectral resolutions.

Over the course of the study, disagreement was found among all of the images in nearly every way cited above. In the effort to explore and analyze the data, we gain an opportunity to look at some of the ways in which remote datasets are normalized and made compatible.

2.3 Image Preparation Processes

2.3.1 Orthorectification and Georegistration

Georeferencing was carried out to verify the compatibility of the Landsat datasets.

The ETM+ was acquired directly from the USGS with a basic level of image processing at L1G. The L1G designation signifies that the image is radiometrically and geometrically corrected to parameters including output map projection, image orientation, pixel grid-cell size, and resampling kernel (USGS, 2007). The correction algorithms model the spacecraft, sensor, focal plane, and detector alignment to improve the overall geometric fidelity. The resulting product is free from distortions related to the sensor (e.g., jitter, view angle effect), satellite (e.g., attitude deviations from nominal), and Earth (e.g., rotation, curvature). The systematic L1G correction process *does not* employ ground control or relief models to attain absolute geodetic accuracy.

The MSS and TM datasets were acquired from NASA's global orthorectified Landsat dataset (also known as GeoCover), the product of a NASA programme conducted to provide an extensive volume of orthorectified and geodetically accurate imagery at high resolution (Tucker et al., 2004). These images have one higher level of processing than then L1G images described above. They are available from the 1970s, circa 1990 and circa 2000, spanning a total of 30 years. The Landsat satellites have the potential to resolve land-cover changes at a resolution of as little as 15m (in the panchromatic

channel of the ETM+), provided that they are orthorectified and geodetically compatible. Because the GeoCover programme was intended to provide geometric and geodetic compatibility, there is thus a general assumption that the GeoCover datasets have consistent, replicated geometry between and among scenes. This compatibility is not assumed among L1G products or between L1G and GeoCover products, as relief displacement can distort the absolute scale.

The ETM+ image, having the best spatial and radiometric resolution, was used as the benchmark reference image in order to avoid compromising the spatial and radiometric data in it. As described above, these two properties are more important than orthorectification, as change detection requires relative geodetic compatibility more than it requires absolute georeferencing. Moreover, most of the analyses were performed using the ETM+ data. Therefore, to ensure that all images were geodetically compatible *with respect to each other*, they were georeferenced to the Landsat ETM+ 1999 image.

Because Landsat images are planimetric, and have a consistent pixel size within each image (Table 2.1), it was decided that a linear transformation would adequately describe any differences between images. To execute the transformation, GCPs were identified among the three images and tied to the ETM+ image. GCPs were recorded so that the standard error of measurement (SEM) could be estimated. The SEM of the sample statistic mean is the estimated standard deviation of the error in the process by which it was generated. The formula is as follows:

$$S_E = \frac{\hat{\sigma}}{\sqrt{n}}$$

Where: $\hat{\sigma}$ = standard deviation of the sample mean

n = sample size

The number yielded represents the residual error term. Two error terms are produced in this case, one for eastings and one for northings.

Based on the results of the linear transformation (refer ahead to Section 3.1.1 for results), it was concluded that an alternative transformation was necessary. The root mean squared error (RMSE) for five other transformations were calculated based on the difference in location of GCPs between the MSS, TM and ETM+ images. The types of transformations were as follows:

i. Linear translation plus homogeneous scale change
ii. Linear translation plus inhomogeneous scale change
iii. Linear translation, rotation, no scale change
iv. Linear translation, rotation, scaling
v. No constraints

Values of the RMSE were then compared and a suitable transformation chosen and manually applied to the image coordinates in ERDAS Imagine. The new image coordinates were calculated based on the type of transformation that was selected. In this case, the RMSE was greatly reduced by a simple linear translation plus homogeneous scaling (LTHS).

The LTHS applies a scaling term and a linear term based on coordinate (GCP) inputs, in the form of:

$$a(x_f) + c$$

Where a is the scaling term and c is the linear shift, applied individually for eastings and northings.

Georeferencing was also carried out for the CORONA satellite images, following procedures laid out by a previous study for DEM generation (Altmaier and Kany, 2004). The procedure uses the OrthoBASE software in ERDAS Imagine.

Airphoto orthorectification is a common procedure applied to airphotos to create planimetric images for interpretation and analysis. This procedure requires several inputs, including the fly height, focal length and interior and exterior orientation of the camera. The interior camera orientation is generally associated with the airphoto fiducial marks, while the exterior orientation is based on the camera viewing geometry. For the CORONA images, interior orientation is not possible to identify, because the images lack fiducials. To compensate for this, nearly a hundred full GCPs (with x, y and z coordinates) were identified for triangulation of the images, using the 1999 Landsat ETM+ image. However, this was not enough for the software to adequately identify the additional tie points required for DEM generation and orthorectification. The residual error measurement of the automatic tie points was too large to execute the orthorectification.

2.3.2 Cloud Detection

The presence of clouds in the 1999 Landsat image was unfortunate, as it obscured a portion of the glaciated terrain below, thereby removing it from this study. Moreover, it brought an added layer of complexity to computation of glacier area.

To find the best distinction between cloud and ground terrain, a combination of statistical and spectral techniques were used. Spectral techniques alone were not enough to detect pixels influenced by clouds. Many pixels show signs that cloud is present over the ground, but in a thin or irregular manner. This allows both clouds and the ground below to send a signal to the sensor, which made it impossible to extract the ground signal from the cloud signal. It's important to know where this is happening, so that it is understood where and when the ground signal is mixed with cloud and where erroneous analysis results may occur.

Cloud detection methods are the same as those intended to detect and classify ground surface features. Many of the methods explained in this section will reappear in a similar form in the later section on snow detection. However, unlike snow and ice studies, there is no single effective index for cloud detection. Thus, various methods were explored, each showing varying degrees of success. They included: principle components analysis (PCA), ratio thresholding, and both supervised and unsupervised classifiers.

Supervised and Unsupervised Classification

This study employed a maximum likelihood[2] test on pixel values to assign a class to each pixel. It can be either trained (supervised) or untrained (unsupervised). Trained classification requires that classes be identified prior to running the classification algorithm. Such classes are normally based on ground truthing or known information about the image. In the case where there is insufficient information about landcover, an unsupervised classifier can be employed in which the classes are self-determined. The number of landcover classes that are expected should be estimated beforehand and used as an input for the classifier. Both types of classifier were attempted for cloud identification. They were not combined with any other method.

Ratio Thresholding

The electromagnetic signature of cloud is distinct from most ground features but is very similar to snow. Divergence of the cloud and snow signature curves occurs in the middle infrared part of the spectrum, corresponding to ETM+ band 5. Over bands 1 – 4, reflectance is high for both snow and cloud, and low in thermal band 6 (because snow and cloud both tend to have low temperatures relative to other features). The curve divergence can be taken advantage of to isolate both snow and cloud.

Although ratio thresholding is a process that is not as automated as supervised and unsupervised classification schemes, it is a basic tool that can be used to identify breaks

2. For more information on maximum likelihood classifiers, see ERDAS Imagine software documentation.

in bimodal or multimodal datasets. It is a simple principle wherein classes are identified based on the histogram distribution of a band ratio. This can generally be used for any image data, whether it is the raw digital numbers or some product of mathematical manipulation. In this case, raw digital numbers were ratioed. I developed a ratio image from Landsat bands 4 and 5:

$$\text{Ratio} = \text{ETM4/ETM5}$$

Where ETM4 is Landsat's Thermal Mapper band 4 (0.525-0.605μm), corresponding to the near infrared (IR), and ETM5 is band 5 (1.55-1.75μm), corresponding to the middle infrared part of the electromagnetic spectrum.

Because clouds are good reflectors of energy in the low channels, it was expected that this ratio would be exceptionally low over cloudy parts of the scene. Similarly, the ratio between any lower band and band 5 could theoretically be used to distinguish clouds and snow from other ground features.

The threshold was applied at a ratio value of sub 0.2, and a cloud mask was produced.

Principal Components Analysis

Principal components analysis was used to visually inspect the ratio threshold image and further eliminate any areas that were cloud covered from the study. This additional measure was used to make sure that areas of thin or irregular cloud were identified as such (see the above discussion on pixels *influenced* by cloud).

Principal components analysis was applied to a subset of the 1999 image in an attempt to highlight snow-cloud differences. The first component characterized the most major differences be the two images, namely, the areas of overall high reflectance and overall low reflectance (which, in effect, produces a contrast image). Not surprisingly, cloud and

snow were grouped into the high end member of the contrast image. It was not until the 4th and 5th components that an obvious distinction between snow and cloud emerged.

Interestingly, an effective cloud detection method emerged from one of the glacier change detection methods. Cloud covered areas were effectively removed from the study area. Each multitemporal MSS, TM and ETM+ band was isolated and transformed via the same LTHS transformation explained previously. They were merged into a monolithic scene using ERDAS Imagine Image Interpreter. The same software was then used to perform a PCA on the image with the hope of detecting spatial changes in glacier size and shape. The desired outcome was not achieved, but the product very clearly identified areas of cloud in the ETM+ image. Ultimately, this PCA image and not the one based solely on the ETM+ 1999 scene was used to manually check and modify the threshold mask.

The PCA image viewed with principal components 1, 4 and 5 served as the benchmark image by which all the other techniques were measured. Principal components 1, 4 and 5 were selected following inspection of the results.

2.4 Analytical Processes

2.4.1 Snow Detection

Several standard snow detection techniques were tried. They can broadly be broken into several groups, summated in Table 2.2.

	Snow Detection Method	Examples	Employed in Studies
1	Thresholding	DN Thresholding	Paul 2000
2	Supervised Classification	none	Paul 2000; Hall et al. 1987, 1995; Bronge and Bronge 1996;
3	Unsupervised Classification	none	Paul 2000; Hall et al. 1987, 1995; Bronge and Bronge 1996
4	Statistical Methods	Principal Components Analysis (PCA)	Hall, D.K. et. al.
5	Snow Indices	Normalized Difference Snow Index (NDSI)	Orheim and Luccitta 1987; Dozier and Marks 1987

Table 2.2 Summary of snow detection methods employed on the Landsat images in this study.

Spectral Normalization

The MSS image has very different spectral resolution from either the TM or ETM+ images which should be apparent from the discussion on the evolution of the Landsat program (refer back to Section 1.3.2). This is problematic for image analysis. The main issue is that different information goes into the classification scheme for the different images. In glacier studies, the only ways to detect snow in MSS images are through a classifier or manual delineation, while ratio methods work better on TM and ETM+ images (Paul, 2002). The two images with greater spectral resolution were reduced to the spectral coverage of the MSS image based on overlapping spectral channels.

Although the Landsat bandwidths have been modified and improved over the decades, there is some overlap in the band channels in the MSS, TM and ETM+ sensors. This overlap was taken advantage of to give the images common spectral resolution. A supervised maximum-likelihood classification was employed on MSS bands 4 through 7 and TM/ETM+ bands 2, 3 and 4. Results of classification on all of the images were then compared.

Ratio Thresholding and Snow Indices

The ratio image created for cloud detection (in Section 2.3.2) also produced a bimodal product from which snow could also be easily identified. The reflectance curve for snow is unique in that it is high in the near IR part of the spectrum (TM/ETM+ band 4), but markedly low in the middle infrared (TM/ETM+ band 5). Therefore, the ratio between the two bands is great over snow. This is such a unique property, in fact, that it effectively separates snow from all other ground cover. The threshold value for the ratio image was placed at 2.0 for snow. Snow masks were then produced for the 1989 TM and 1999 ETM+ scenes.

The normalized difference snow index (NDSI) (Kyle et. al., 1978; Dozier, 1984; Dozier, 1989) employs a property of snow similar to that of the ratio thresholding technique. In this case it uses band 2 instead of band 4, although it is again based on the reflectance disparity between two bands:

$$NDSI = (ETM2 - TM5)/(ETM2 + TM5)$$

Where TM2 is Landsat's Thermal Mapper band 2 (0.525-0.605μm), corresponding to visible green light, and TM5 is band 5 (1.55-1.75μm), corresponding to the middle infrared. Again, as in the near IR, snow effectively reflects green light.

Both of these techniques produced similar results. However, because the former achieves slightly better results over dirty snow and ice and is marginally quicker to use, it was used.

Supervised and Unsupervised Classification

This is the same technique used for cloud detection (refer to the description in Section 2.3.2), only in this case the target was glacier ice.

Statistical Methods

A principal components analysis was performed on the images in an attempt to isolate snow. Each image was processed with the ERDAS Imagine PCA model. The results showed little promise for snow detection, especially in the ETM+ image where cloud was present. The first few components were not able to separate snow and cloud, and the last few components only picked up the noise signal from the images. The middle components showed better snow and cloud discrimination, but were not useful for identifying debris-covered glacier ice.

2.4.2 Areal Snow Extent Measurements

Areal snow extent measurements for 1978, 1989 and 1999 were taken from the products of the processes described above. The results of the snow detection methods were, in all cases, binary grids. These binary grids were produced in ERDAS Imagine and carried over to ArcGIS for conversion into vector data. Grid values equal to 1 represented snow. The ArcGIS Spatial Analyst was used to identify grid cells with a value of 1 and convert them into polygonized vector data. I then cleaned up the polygons with the editor feature (i.e. eliminating very small snow patches and erroneously classified pixels). Because the TM and ETM+ scenes were adjacent WRS scenes (and the MSS scene was from the first generation WRS), there was a slight difference in the area covered by each of them. The very far eastern part of the study area was not captured in the ETM+ and MSS images, while the very far western part of the image was not captured by the TM image. Therefore, additional cleaning of the polygons was required to remove the very far eastern and western parts of the snow masks before snow extent and area measurements could be compared. The problem could have been easily have overcome if the side-by-side WRS scenes were acquired. However, of the four (1977, 87, 89 and 99) Landsat images available for the area during the desired time of year, not one was available with the neighbouring east or west image.

Measurements for the total extent of snow in 1971 were inferred from the combined results of the snow extent measurements from 1989 and 1999 and measurement of the terminus positions in the 1971 photographs. For these measurements, it was assumed that the total area of glacier change between 1971 and 1999 occurred at the terminal margins of the glaciers. Average widths for the termini in each of the valleys were measured and multiplied by the amount of estimated retreat of the terminus between the images. Because terminus fluctuations were not measured on all glaciers, changes in the overall amount of snow cover could not be calculated. However, I took an estimation of the total snow area lost from all glaciers that were included in the terminus analysis.

2.4.3 Terminus Measurements

The terminus position was measured for all possible glaciers. These measurements were taken wherever the terminus was visible in both the 1971 CORONA image and the 1999 Landsat image.

There were two things that precluded the possibility of terminus measurements. The first was cloud cover in the 1999 image. The other images are all cloud-free. Although they provide a clear view of every glacier in each image, the acquisition dates were not appropriate for a study of sufficiently contemporary conditions. The second, interestingly, was also a deficiency in the Landsat images, and not the CORONA imagery. Because the Landsat WRS footprint is split over the Central Caucasus, two images for each date would be required to cover the entire study area. Though the area lost at the margins of the images is small, there is still some loss of information. In the east, Devdorak, Abano and Ortisveri glaciers could not be measured. However, for reasons we will see later, this is not crucial to analysing the glacier – climate dynamic.

Data for terminus positions, as previously mentioned, was collected for only two dates, 1971 and 1999. CORONA images were analysed by air photo interpretation. In this case, both digital and hard copies of the images were used in interpretation of the terminus position. The benefits of digital photographs were enormous. The images could be

enlarged very quickly and various stereopairs easily produced by simply making print copies.

Landsat images were much more difficult to interpret, especially before I had gained an appreciation of the terrain that I was looking at. The biggest problems in interpretation were at the glacier termini, where there was the greatest collection of debris. CORONA photographs aided in identifying the general shape of each glacier terminus in Landsat images.

Automated (as opposed to manual) methods were the first employed on the images, and this occurred during the snow detection procedure. At that point I was hopeful that glacier termini would be automatically detected with reasonable accuracy through snow and ice detection indices and other methods, particularly since glaciers immediately to the west were described as clean and virtually debris-free. Unfortunately, good, sharp lines and clear terminus delineations did not materialize from any of the automated procedures. It was clear that a manual approach would be required. This made the process many times longer and more difficult.

I've emphasized that before the airphotos were available, detecting some glaciers was virtually impossible. I'd like to highlight the fact that if some glaciers are difficult to detect at all, then termini (resolved at only a few pixels) are ever more so. For some glaciers it was less a problem and for those ones measurements are much more reliable. Where ambiguity in interpretation exists, I've applied error bars to the measurements.

Although many of the glaciers are simply difficult to interpret just by their nature, there were a few things that eventually made the process much easier. The first is comparison with the airphotos. Because of the great level of detail in the images and the fact that they are stereopairs, information about the landscape and the processes acting on it became clear. From this information, direct comparisons could then be made between the airphotos and the 1999 Landsat image in order to help interpret the scene. This was

particularly useful where there was not enough spectral or spatial resolution to identify features.

A second thing that aides in Landsat interpretation is the fact that vast spectral information is carried in the ETM+ images. The airphotos have fine spatial resolution, but it is carried entirely in panchromatic black and white film. The ETM+ provides several bands (discussed earlier). The information carried in each band is different, and ground objects often produce a different signal in different bands. These differences are useful in distinguishing objects from one another. By viewing different band combinations, different features could be highlighted. For example, the bands corresponding to the visible part of the spectrum (bands 1, 2 and 3) show minimal variability between the ablation zone of glaciers and adjacent valley walls in the 1999 image, particularly nearer to the terminus. However, the inclusion of bands 4 and 5 highlights areas there is ice (see Sections 2.3.2 and 2.4.1 for a discussion of the spectral reflectance curve for ice), and therefore where glacier may be present. Many of the terminus measurement figures in this report were produced using bands 4 and 5 to illustrate this point.

2.4.4 Climate Trend Analysis

To tie the results of the previous sections together and contextualize them in terms of climate, real climate data needed to be gathered and analysed. The motivation behind acquiring the climate data was to attempt to identify trends or events over the period 1971 – 1999 that might help explain the observed glacier behaviour. The analysis began with a strict look at the climate data for the Eastern Central Caucasus Mountain region, but was later extended based on preliminary results and research.

Climate data were provided by the Climate Research Unit (CRU) at the Tyndall Centre for Climate Change Research (CRU datasets' web address: http://www.cru.uea.ac.uk/cru/data/hrg.htm, accessed March 2007). Specifically, the datasets used are global grids of major climate indicators at 0.5deg resolution, known as CRU TS 2.1 (Climate Research

Unit Time-Series dataset 2.1). Climate variables in this dataset are either primary or secondary, and all are monthly time-series from 1901-2001. The primary variables (precipitation, temperature and diurnal temperature range) were interpolated directly from meteorological station observations. Only the first two were used in this study. The secondary variables available from CRU TS 2.1 are wet-day frequency, vapor pressure, cloud cover, and ground frost frequency. These were produced from a combination of direct observations and synthetic data estimates through predictive indicators from the primary variables (New et al, 1999). No secondary elements were incorporated in this study. All data are normalized such that the station data was in agreement in terms of space and time (New et al, 1999).

Weather station data often show correlation with weather conditions at nearby glaciers (Oerlemans, 2002), provided that the glaciers respond in a regular way to climatic changes. The CRU data uses the weather stations nearest to each half-degree grid cell to determine the values of climate variables within each cell. Therefore, I believe that the CRU data gives a good approximation of conditions at glaciers within the cell, and can help explain glacier behaviour.

The actual CRU data are large ASCII files. They are, as noted, monthly time-series from 1901-2001, grouped by annum and headed by a cell reference, which has a corresponding lat-long reference. The areas for which climate data were required were identified in lat-long coordinates and translated to corresponding cell references for lookup. The climate data was extraxcted and reformatted for analysis.

Initially, average monthly temperatures were taken together to yield an annual average temperature to be used as an input for time-trend analyses. This was later modified to focus on temperature trends between successive melt seasons. While average annual temperature gives an impression of conditions for the year on the whole, (and from that, of the temperature trend over time) the values mask seasonal variability. Annual temperatures used in trend analysis were deceptive because of this. The accumulation and ablation season are primarily influenced by different variables over the course of the

mass balance year. During the accumulation season, it is primarily precipitation that controls the rate and level of snow accumulation. In the simplest case, during the winter, when the temperature remains below zero, all precipitation can be expected to fall as snow. During this period temperature has no direct control on the actual amount of accumulation, provided that it remains negative. Conversely, during the ablation season, the most significant control on ablation is temperature. Higher positive temperatures result in a greater amount of energy available to melt snow. The months during which ablation is most likely to occur (in the case of the Caucasus, May-Sept) give a good indication of the amount of energy available to melt snow at the surface. Thus, a warming or cooling trend during the time of the year when temperatures are positive will produce either more or less energy to melt snow over time, respectively.

Alternatively, because the data are divided by month, data for specific mass balance years could be investigated; though such an analysis was not performed here.

2.4.5 Comparative Climate Trend Analysis

Time-series trend analyses were performed on climate variables for 9 glaciated regions of the world; paralleling focus areas from a World Glacier Monitoring Service (WGMS) study on world glacier fluctuations (Zemp et al. 2004). The areas are as follows: Cascade Mountains, Alaska, Andes, Svalbard, Scandinavian Peninsula, Alps, Altai, Caucasus and Tien Shan. The selected group provides a diverse representation of physiography, latitude, climate and glacial regime with which to compare the Caucasus. However, it is the climate - mass balance relationship with which we are most concerned. The question raised here is whether or not climate variables account for - at least in part - significant differences in glacier behaviour observed between these areas.

Differences between Caucasus and Alpine glacier behaviour are of special interest as both the latitude and physiography of the two areas are similar. This was recognized even in early years of scientific investigation in the Caucasus, as that time was characterized by an apparent tendency to draw parallels between that region and the Alps (Horvath and

Field 1975). This is not surprising, as early scientific undertakings lacked any kind of real, scientific background information. The only available, *direct* sources would have been historic and piecewise information from inhabitants and travellers. Thus, a natural starting point would have been comparative analysis with a much better-studied, familiar area.

Other analyses are supplementary, and are intended to contextualize the behaviour of the Caucasus in terms of worldwide glaciation.

2.4.6 Djankuat Glacier Mass Balance and Climate Implications

Djankuat Glacier is the only glacier located in the Central Caucasus that receives annual attention as a target for mass balance measurements. Located at approximately 43°12'N, 42°46'E, like most Caucasus glaciers it is on the north flanks of the range and feeds into its valley in a northwesterly trend (Figure 2.0). Mass balance measurements are available for a 40-year time-series, 1967-1997.

This data is intended to supplement the discussion of glacier behaviour and climate change by supporting (or debunking) observations and interpretations. It is also used to provide evidence that should help describe the climatic regime and illustrate the general nature of the glaciers in the Caucasus. It is particularly helpful in making more concrete statements about the interaction between Caucasus glacier behaviour and climate in light of the findings of the Caucasus climate trend analyses.

The assumption in using mass balance data is that the glacier can be treated as a kind of weather station that registers climate fluctuations and gives direct insight into prevailing climate change. Recorded temperatures from Djankuat show a correlation with recorded temperatures at the Terksol weather station, 17kms to the southeast. The correlation is very high at 0.82 (Shahgedanova, 2005). It follows that Djankuat data realistically represents the local climate, and will be used from time to time as a representation of such.

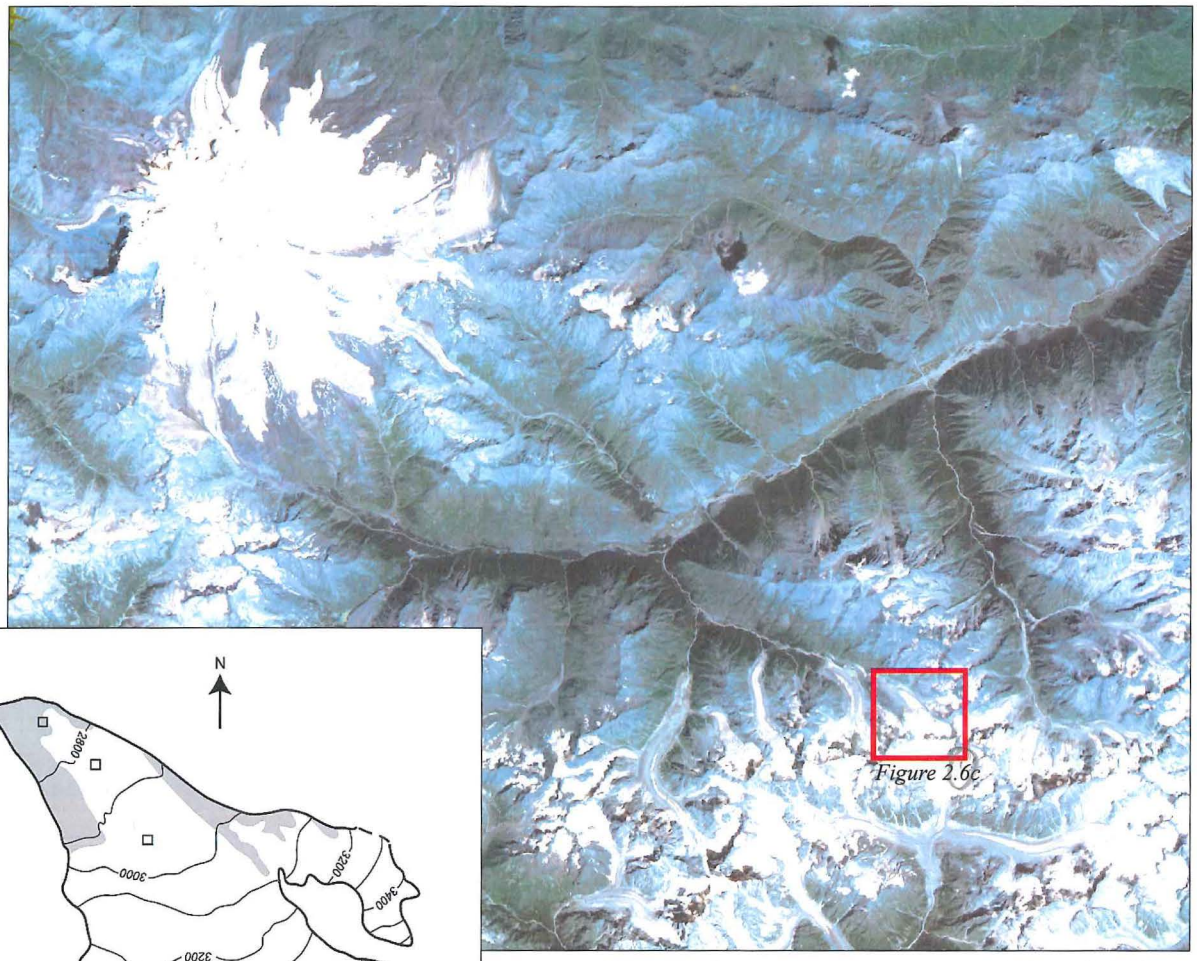

Figure 2.0b Mt. Elbrus Region and Djankuat Glacier

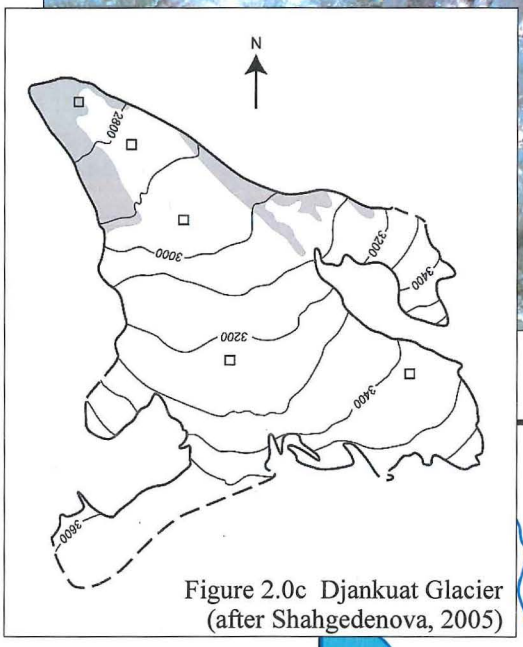

Figure 2.0c Djankuat Glacier
(after Shahgedenova, 2005)

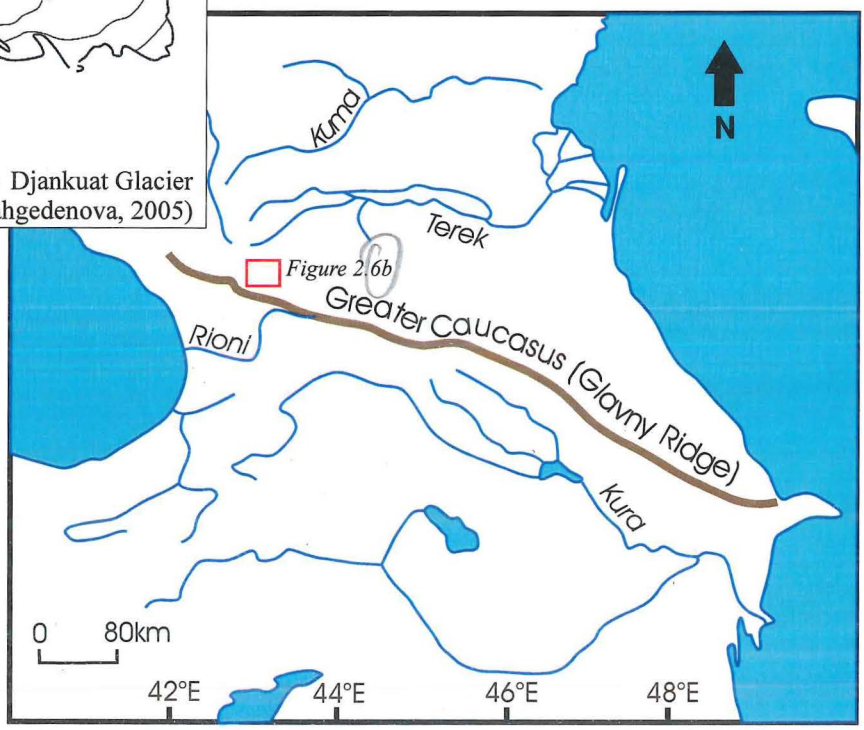

Figure 2.0a Caucasus Region (after Shahgedenova, 2005)

CHAPTER 3

RESULTS

3.1 IMAGE PREPARATION PROCESSES

3.1.1 Image Orthorectification and Georegistration

Georeferencing techniques were applied to both the Landsat images and the CORONA satellite images. There was great success in making the Landsat images geodetically compatible; however, there was little success with the CORONA images.

The first transformation applied to the MSS and TM images was a simple linear shift based on the location of ground control points (GCPs) described in Section 2.3.1.

The overall results of the MSS linear transformation were unsatisfactory, particularly in the eastern reaches of the image where the number of GCPs was necessarily less than in the west because of cloud cover. Persistent and eastwardly diverging offsets were observed (Figure 3.0). The geometry of the offsets is described in the graph inset in Figure 3.0 and the corresponding table. Offsets are greater for the eastings than northings and greater in the east than in the western part of the image.

Based on the results of the first transformation, we could deduce that these two images were not geodetically compatible in a linear respect with each other. This is not surprising when the different levels of image pre-processing are taken into account. While the MSS image is terrain-corrected, the ETM+ image not.

The second transformation was faster and more streamlined, as many ground control points had already been identified and established. Moreover, the TM image had much better resolution than the MSS image, so existing GCPs were quickly identified and many more added to their ranks. Again, a linear shift was applied, and the results were very similar to the first transformation (Figure 3.1). The direction and magnitude of the offsets was similar to that observed in the MSS image (see Figure 3.1 graph and table inset).

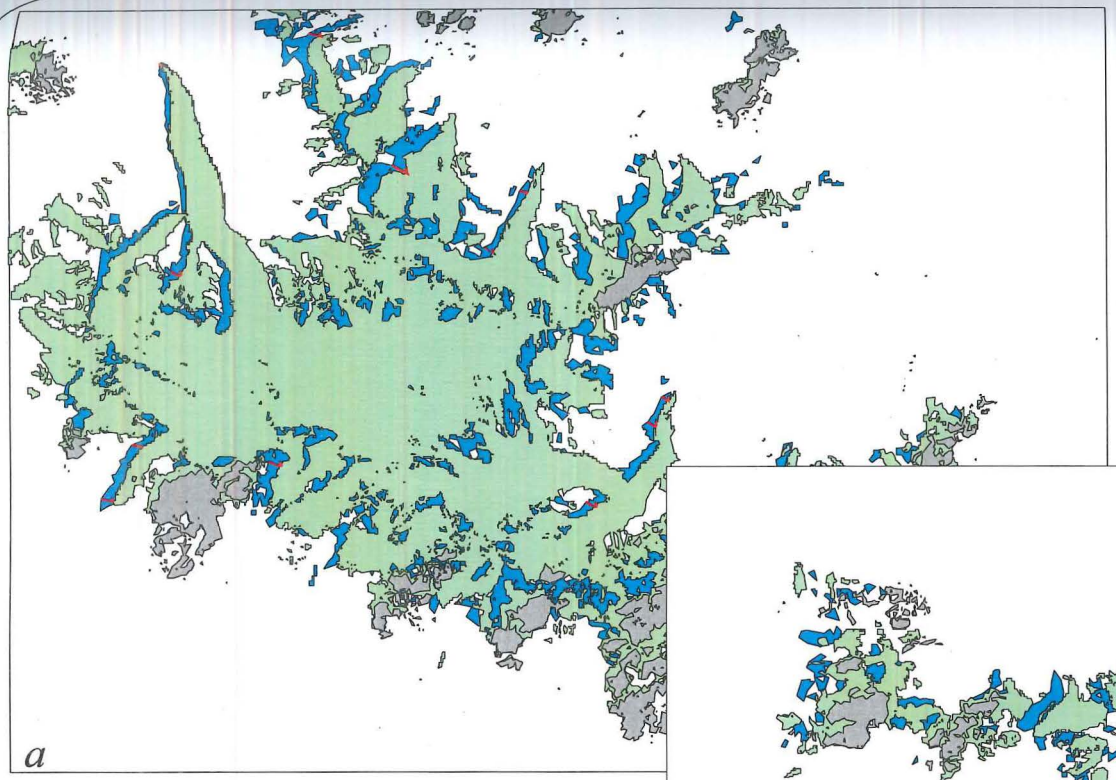

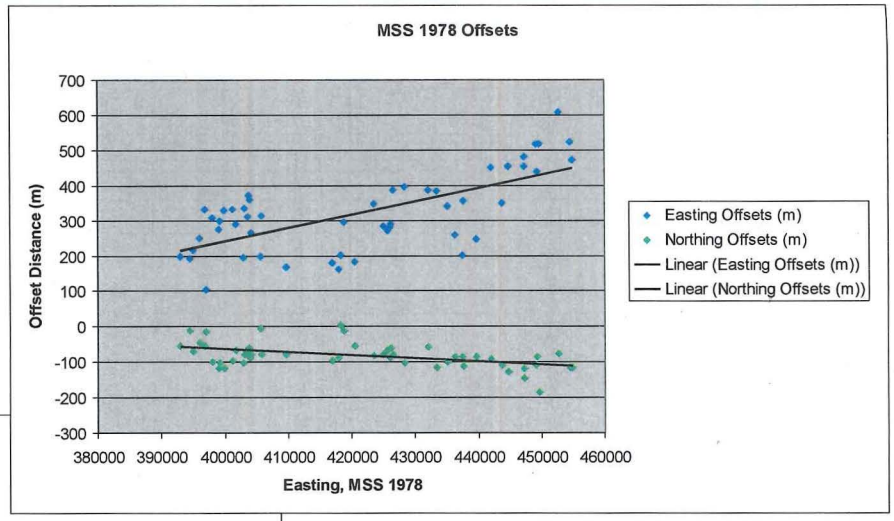

Graphical representation of GCP offsets from west to east in the study area. Note the increase in offset values with eastward migration.

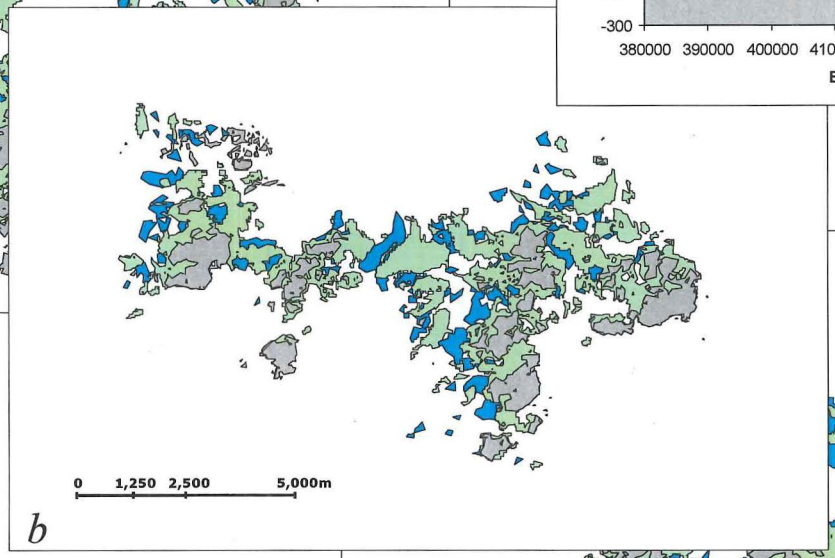

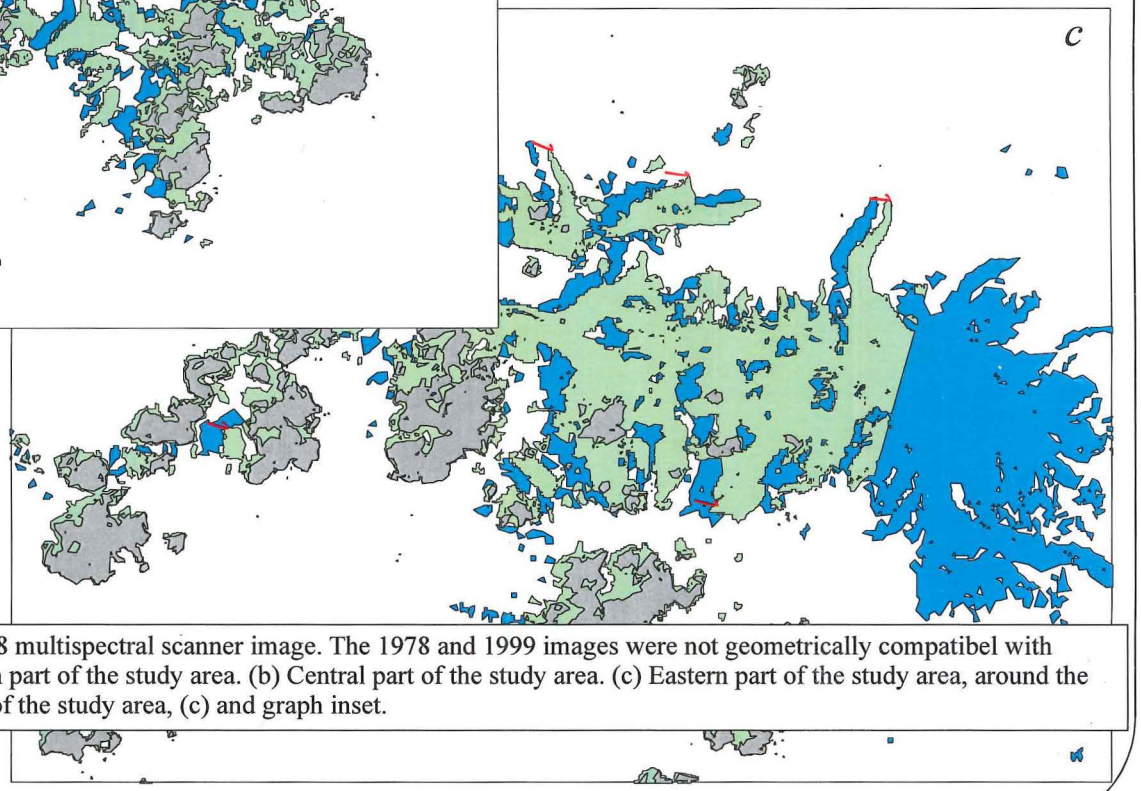

Glaciated area, 1999 (supervised classification)
Glaciated area, 1978 (supervised classification)
Cloud cover, 1999

	Eastings	Northings
Multispectral Scanner, 1978		
Average gcp offset, West	269	-71
Average gcp offset, Central	330	-76
Average gcp offset, East	479	-116

Average GCP offsets between the 1978 MSS image and the 1999 ETM+ image

Figure 3.0 Snow masks developed from image processing of the non-georeferenced 1978 multispectral scanner image. The 1978 and 1999 images were not geometrically compatibel with each other, which resulted in the observed divergence of the two snow masks. (a) Western part of the study area. (b) Central part of the study area. (c) Eastern part of the study area, around the Mt. Kazbek massif. The observed offsets are greater in magnitude in the eastern reaches of the study area, (c) and graph inset.

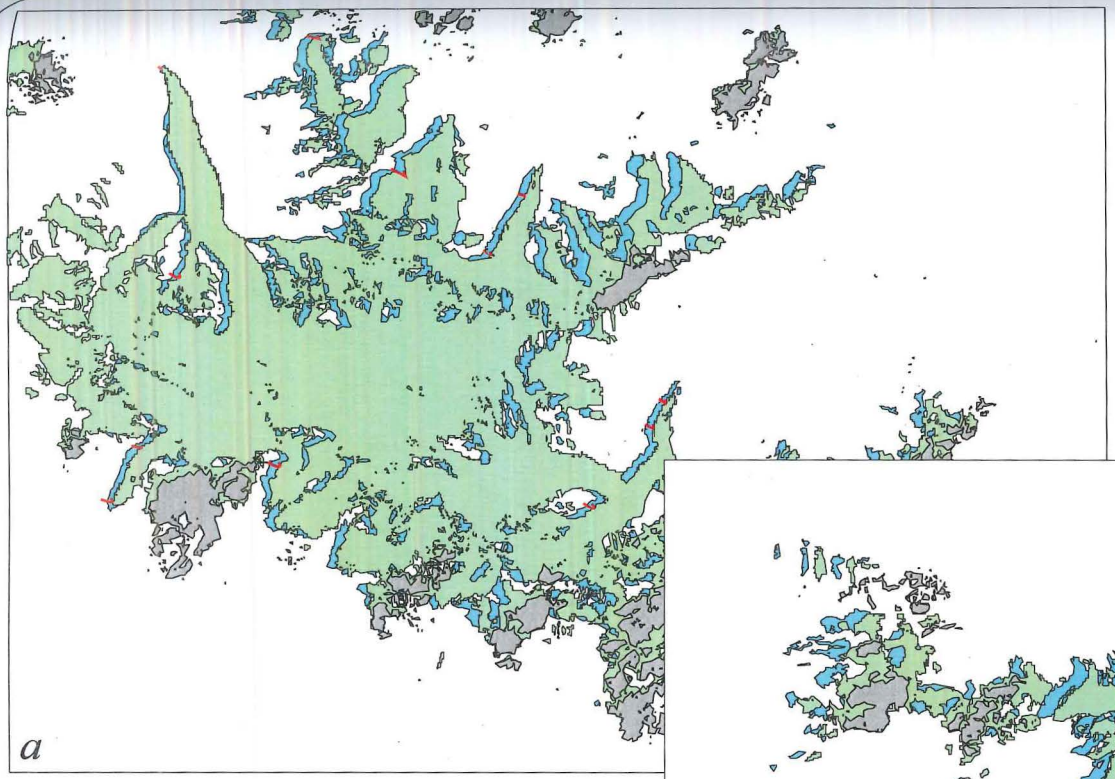

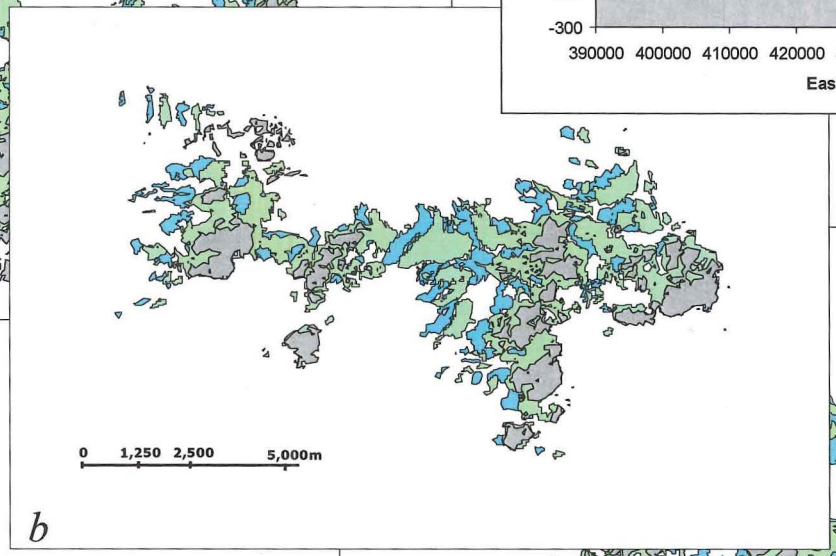

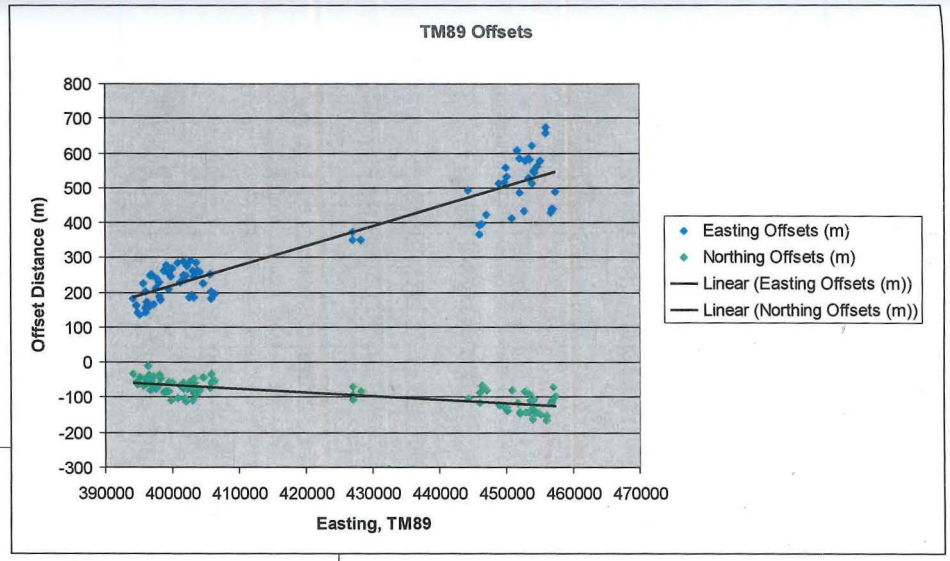

Graphical representation of GCP offsets from west to east in the study area. Note the increase in offset values with eastward migration.

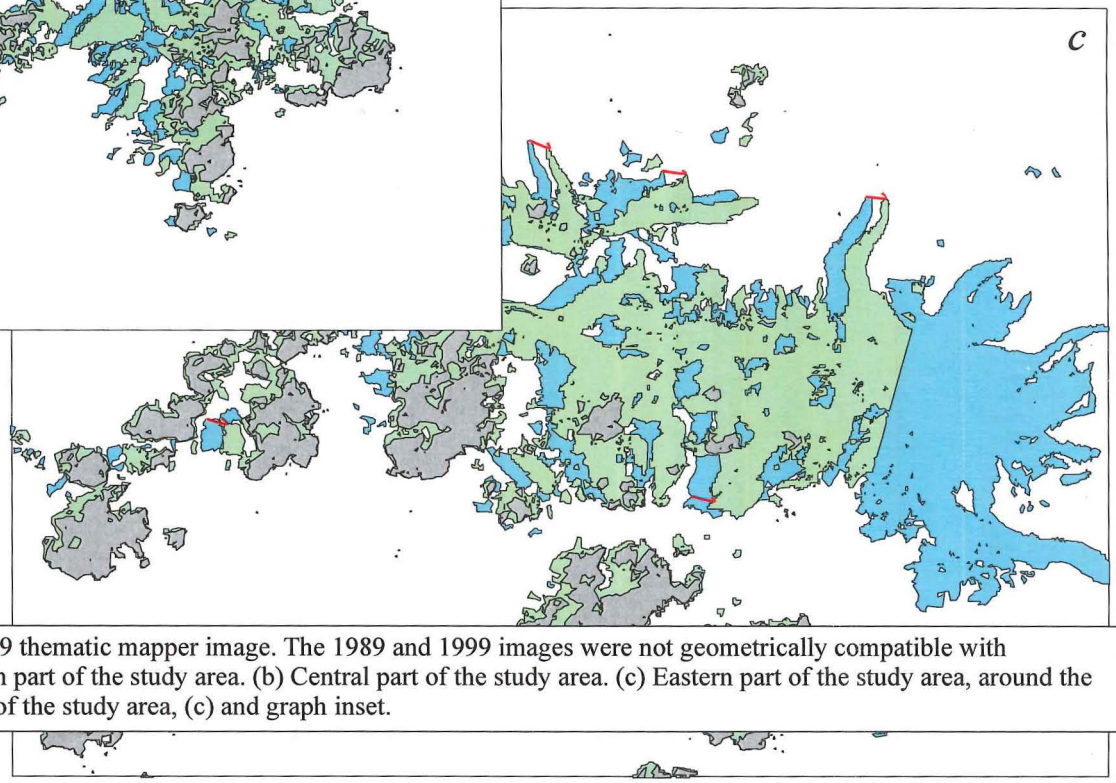

a

b

c

Glaciated area, 1999 (supervised classification)
Glaciated area, 1989 (supervised classification)
Cloud cover, 1999

	Eastings	Northings
Thermal Mapper, 1989		
Average gcp offset, West	219	-64
Average gcp offset, Central	362	-87
Average gcp offset, East	516	-118

Average GCP offsets between the 1989 Tmimage and the 1999 ETM+ image

Figure 3.1 Snow masks developed from image processing of the non-georeferenced 1989 thematic mapper image. The 1989 and 1999 images were not geometrically compatible with each other, which resulted in the observed divergence of the two snow masks. (a) Western part of the study area. (b) Central part of the study area. (c) Eastern part of the study area, around the Mt. Kazbek massif. The observed offsets are greater in magnitude in the eastern reaches of the study area, (c) and graph inset.

At this stage, the images were overlaid atop each other and a visual check performed to confirm the results of Figures 3.0 and 3.1. Indeed, this confirmed that even after the linear transformation was applied, the MSS and TM images were compatible with each other, but not the ETM+ image. It was maintained that the ETM+ image would be the benchmark image because it was the most recent (and would therefore be used more often than the other images in the analytical procedure of glacier behaviour) and had best radiometric and spatial resolution.

The results of the two transformations motion to a peculiarity among the images: both of the earlier images were incompatible in a geometrically consistent way with the later image. Therefore, it seemed reasonable that a different geometric transformation might produce adequate image compatibility. Additionally, the differences between the GeoCover datasets and the L1G dataset could probably be described by the same geometric correction and be applied to both.

The five transformations described in Section 2.3.1 were assessed for suitability based on the locations of the GCPs. The RMS errors for each transformation are summarized in Table 3.0. The best results, by far, were transformations involving scale readjustment. Because all four scaled transformations (**i, ii, iv** and **v**) give similar RMS errors, the simplest one (LTHS) was selected and applied to the MSS and TM images based on the equation, $a(x_f) + c$ from Section 2.3.1.

A visual check on the newly applied transformation suggested a good fit and good compatibility among the three images. The process of snow detection was what ultimately confirmed this however, since the snow detection masks showed no offsets like the ones exhibited in Figures 3.0 and 3.1.

TRANSFORMATION	RMSE
Linear translation only	108.06
Linear translation plus homogeneous scale change	81.85
Linear translation plus inhomogeneous scale change	81.15
Linear translation, rotation, no scale change	108.04
Linear translation, rotation, scaling	81.63
No constraints	79.16

Table 3.0 Root mean squared error results describing the fit of six different transformations to the GCPs identified for the MSS and TM images.

3.1.2 Cloud Detection

Supervised and unsupervised maximum-likelihood classifiers consistently grouped cloud and snow together. This was probably because of the similarities in the reflectance signatures of snow and cloud in the first four ETM+ bands. There was a similar problem over other areas of high reflectance, which indicated that classifiers are not useful for cloud detection, because of the similarity of the digital numbers in many of the bands.

The ratio thresholding technique proved to be more successful, though it too had drawbacks. The biggest problem with the ratio image was not so much that snow and cloud could not be differentiated (it could, and very easily), but that the ratio threshold grouped some ground areas into the cloud mask. These areas tended to be at elevations high in the mountains. Cloud and mountain terrain have clear textural differences, so the high mountain zones were identified as such. They could be isolated and deleted from the cloud mask, particularly with the aide of the PCA image.

The final ArcGIS shapefile output of the cloud detection process is illustrated in Figure 3.2. Clouds were a major hindrance to the actual analysis process, effectively eliminating approximately 8.82km^2, or 6.6% of the total estimated 1989 glacier area and 15.08km^2, or 8.0% of the total estimated 1978 glacier area from analysis. Figures are not available for the amount of glacier area that was removed from the 1999 image, for the fairly obvious reason that glaciers beneath the clouds could not be measured.

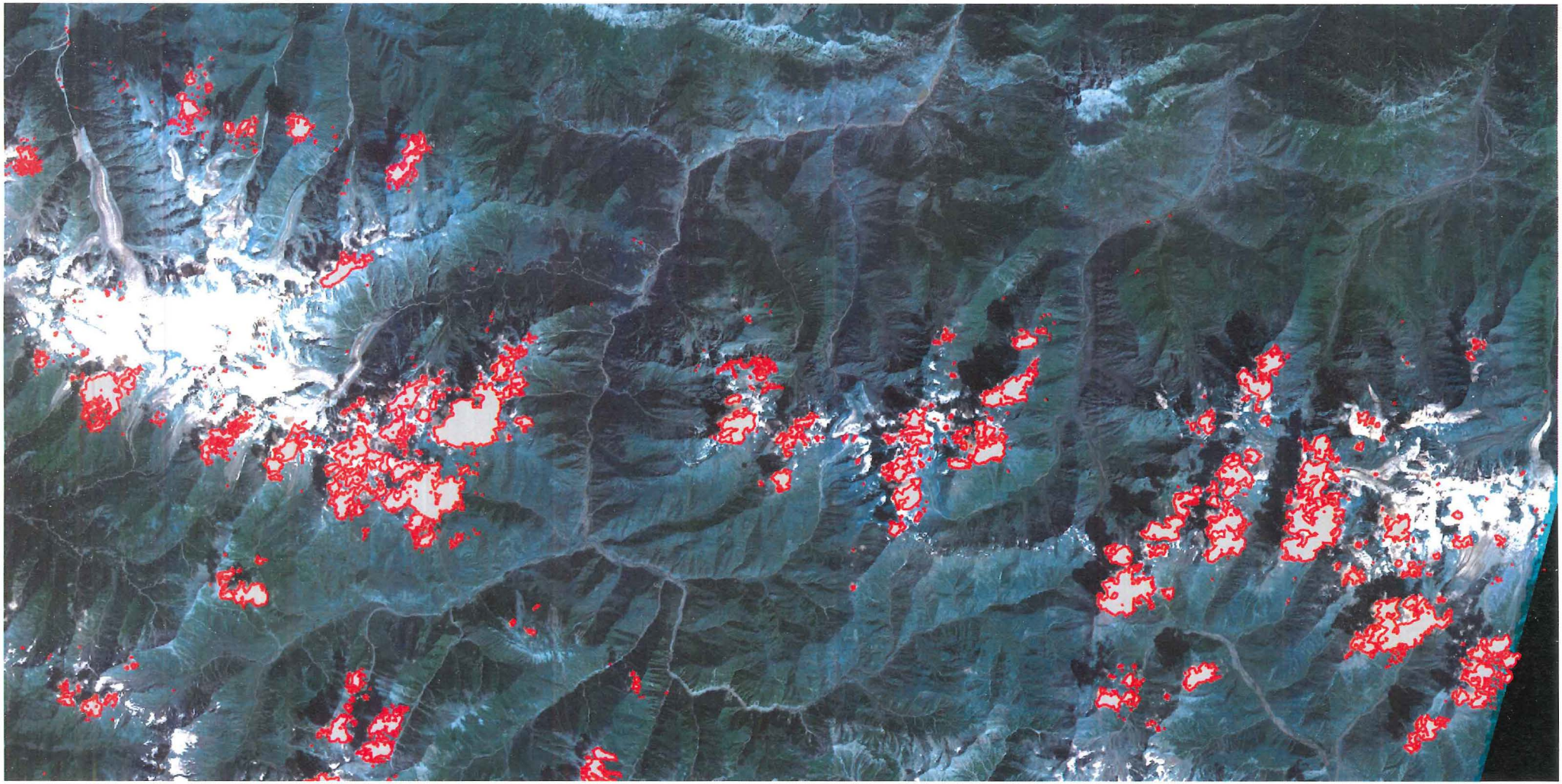

Figure 3.2 Landsat ETM+ 1999 image with cloud mask. The red lines delineate the presence of cloud in the image.

The biggest problem areas were at places where clouds covered the ablation zone, especially the termini of glaciers. This was the case for the Midagrabin Glacier, which is one of the few glaciers on the Mt. Kazbek massif that respond regularly to climate fluctuations and not the activity of the mountain. And so it was a shame.

Despite the obvious shortcomings of using an image with cloud cover, a few valuable things were achieved. The first was determining two good processes through which clouds could be detected. The ratio technique was a fast way to eliminate suspected cloud cover and ensure that all snow and ice covered terrain remained. The PCA image was indispensable for visual and manual interpretation of cloud cover. The one shortcoming is that it was ultimately time-consuming. More work with the PCA image might have been useful to make cloud delineation via PCA automated.

The second thing was an explanation for the vast differences in snow area between 1978 and 1999. At first, there was a great deal less snow calculated in 1999 than in 1978 or 1989, but when the cloud mask was applied to the 1978 and 1999 images, the difference in area was reduced. To clarify: the cloud mask was *subtracted* from the 1989 and 1978 glacier masks to produce new glacier masks with reduced areas (Figures 3.3 through 3.7 illustrate the process). Calculations of glacier area from images that did not have cloud in them were far greater than the 1999 image that contained a great deal of cloud, because not all glaciated terrain was identified in 1999. Removing cloud-covered areas from all scenes rectified the problem.

3.2 Analytical Processes

3.2.1 Snow Detection: Spectral Normalization

The overall effect of reducing the number of spectral bands in order to normalize the data was a loss of crucial information.

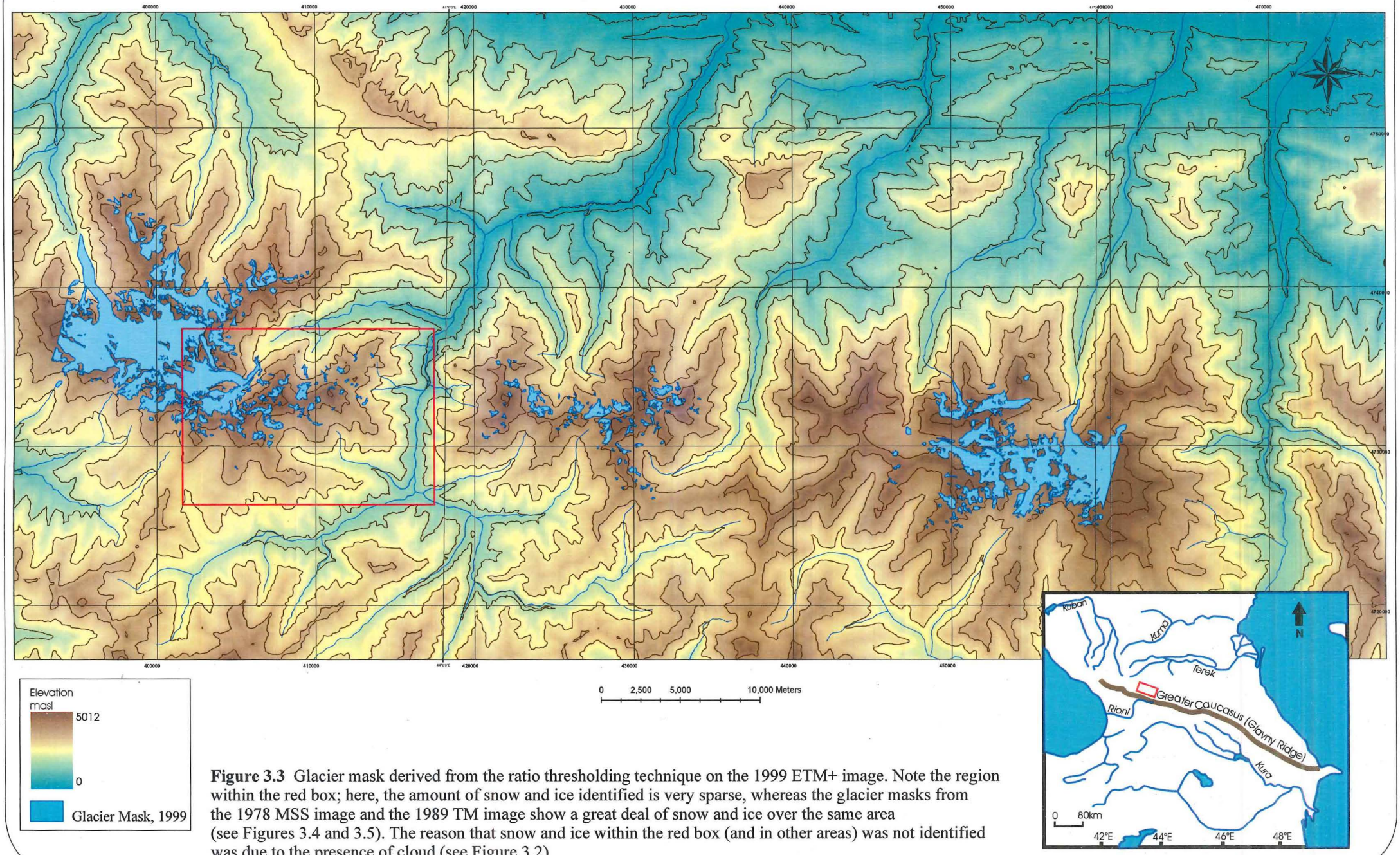

Figure 3.3 Glacier mask derived from the ratio thresholding technique on the 1999 ETM+ image. Note the region within the red box; here, the amount of snow and ice identified is very sparse, whereas the glacier masks from the 1978 MSS image and the 1989 TM image show a great deal of snow and ice over the same area (see Figures 3.4 and 3.5). The reason that snow and ice within the red box (and in other areas) was not identified was due to the presence of cloud (see Figure 3.2)

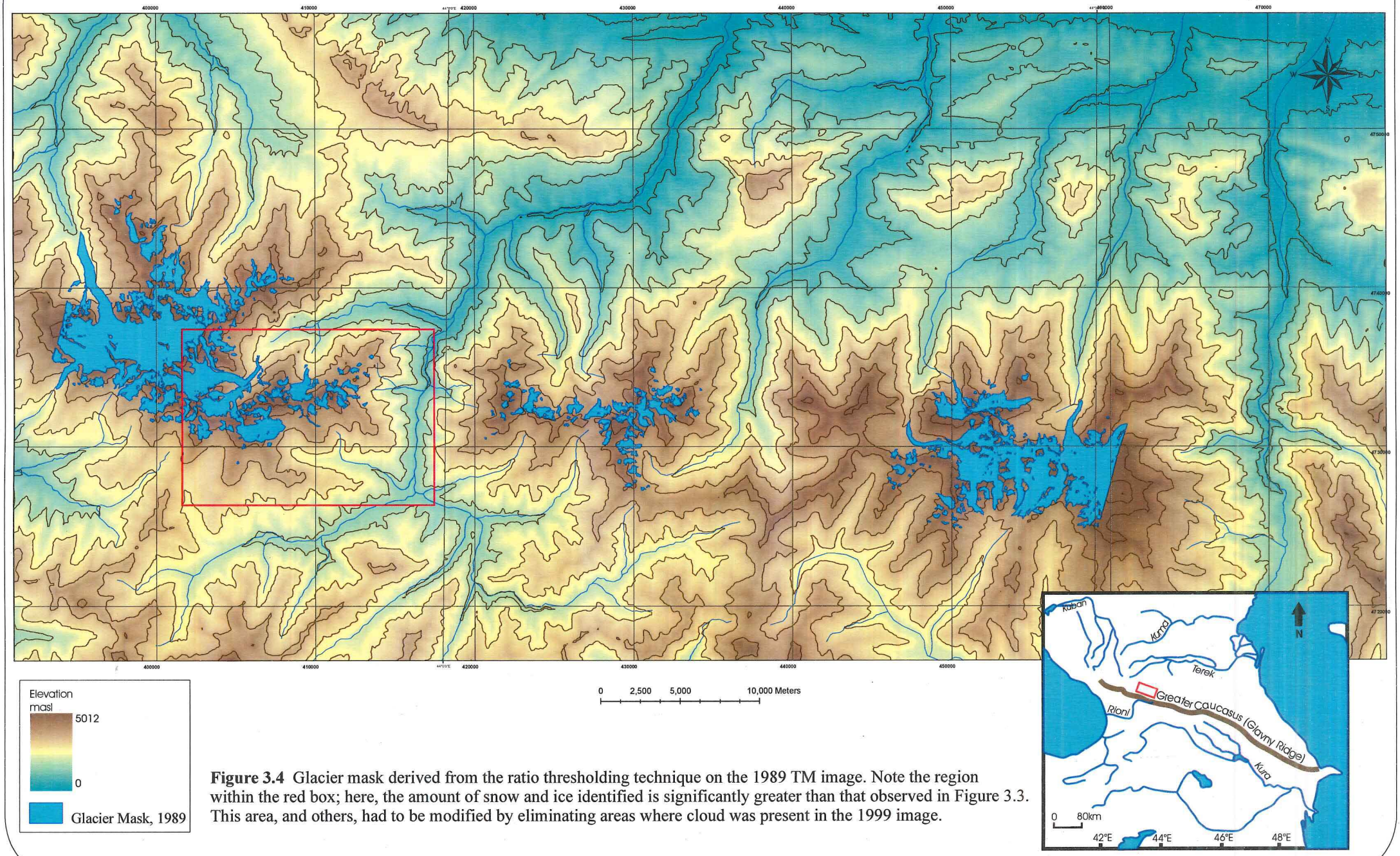

Figure 3.4 Glacier mask derived from the ratio thresholding technique on the 1989 TM image. Note the region within the red box; here, the amount of snow and ice identified is significantly greater than that observed in Figure 3.3. This area, and others, had to be modified by eliminating areas where cloud was present in the 1999 image.

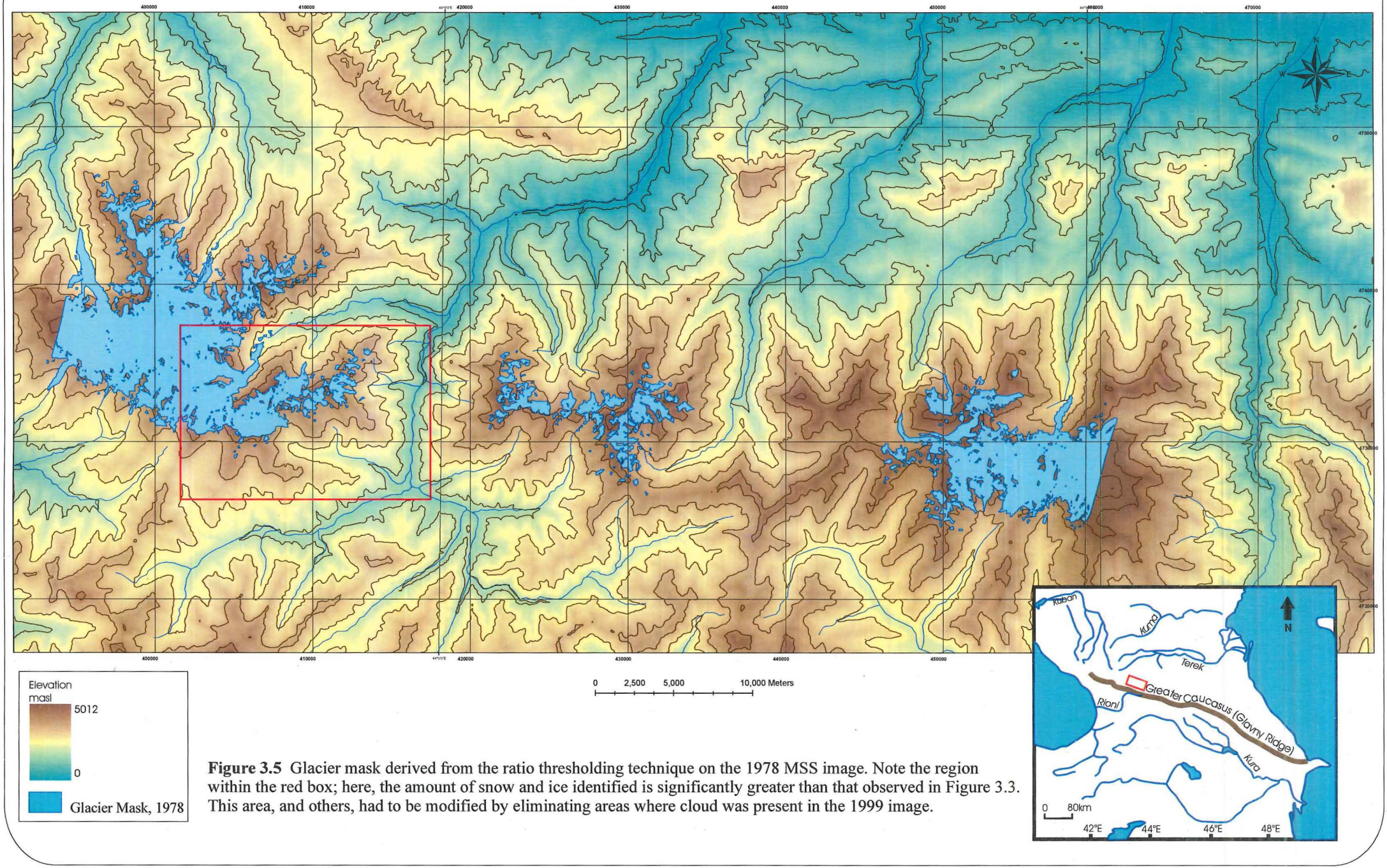

Figure 3.5 Glacier mask derived from the ratio thresholding technique on the 1978 MSS image. Note the region within the red box; here, the amount of snow and ice identified is significantly greater than that observed in Figure 3.3. This area, and others, had to be modified by eliminating areas where cloud was present in the 1999 image.

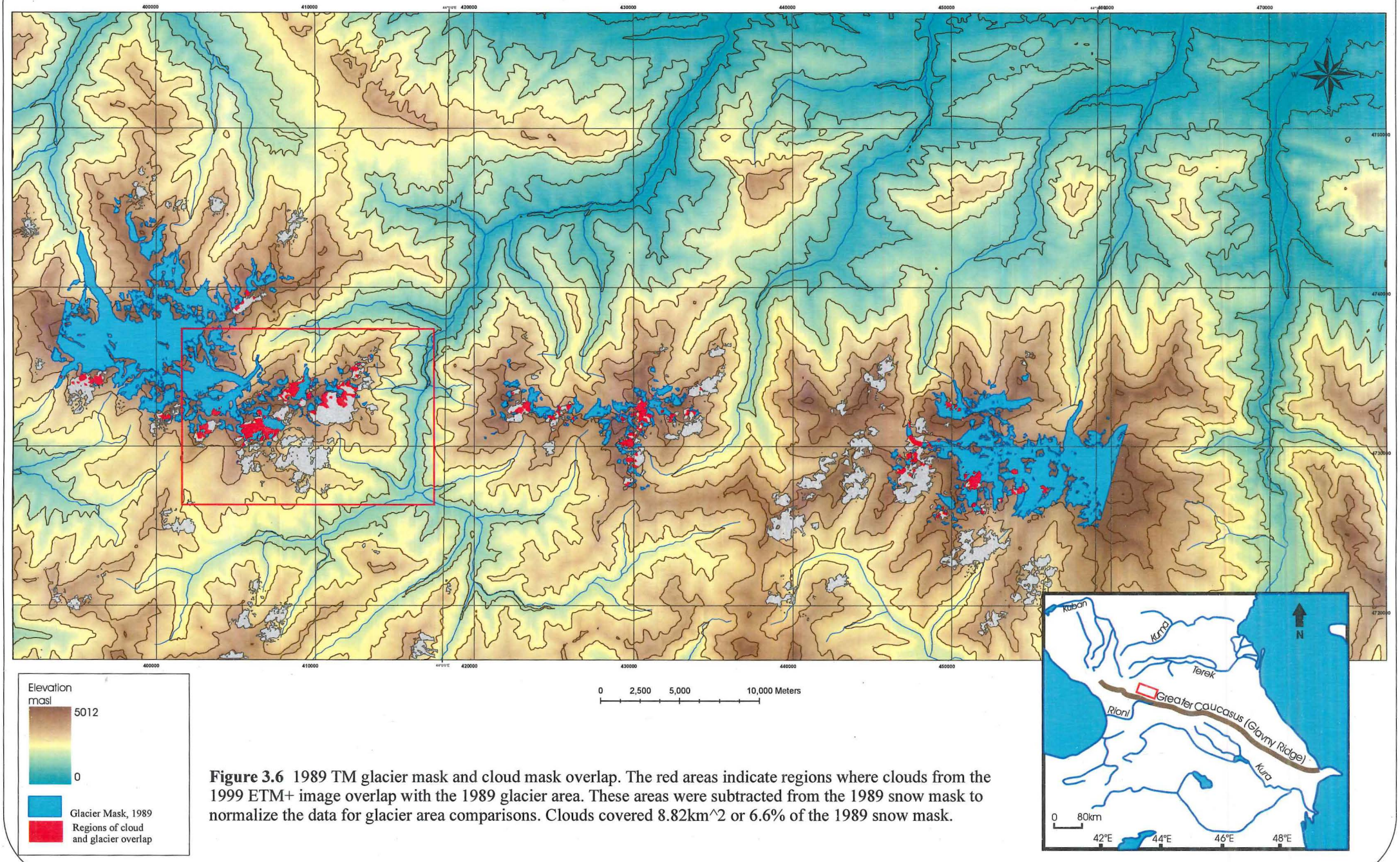

Figure 3.6 1989 TM glacier mask and cloud mask overlap. The red areas indicate regions where clouds from the 1999 ETM+ image overlap with the 1989 glacier area. These areas were subtracted from the 1989 snow mask to normalize the data for glacier area comparisons. Clouds covered 8.82km^2 or 6.6% of the 1989 snow mask.

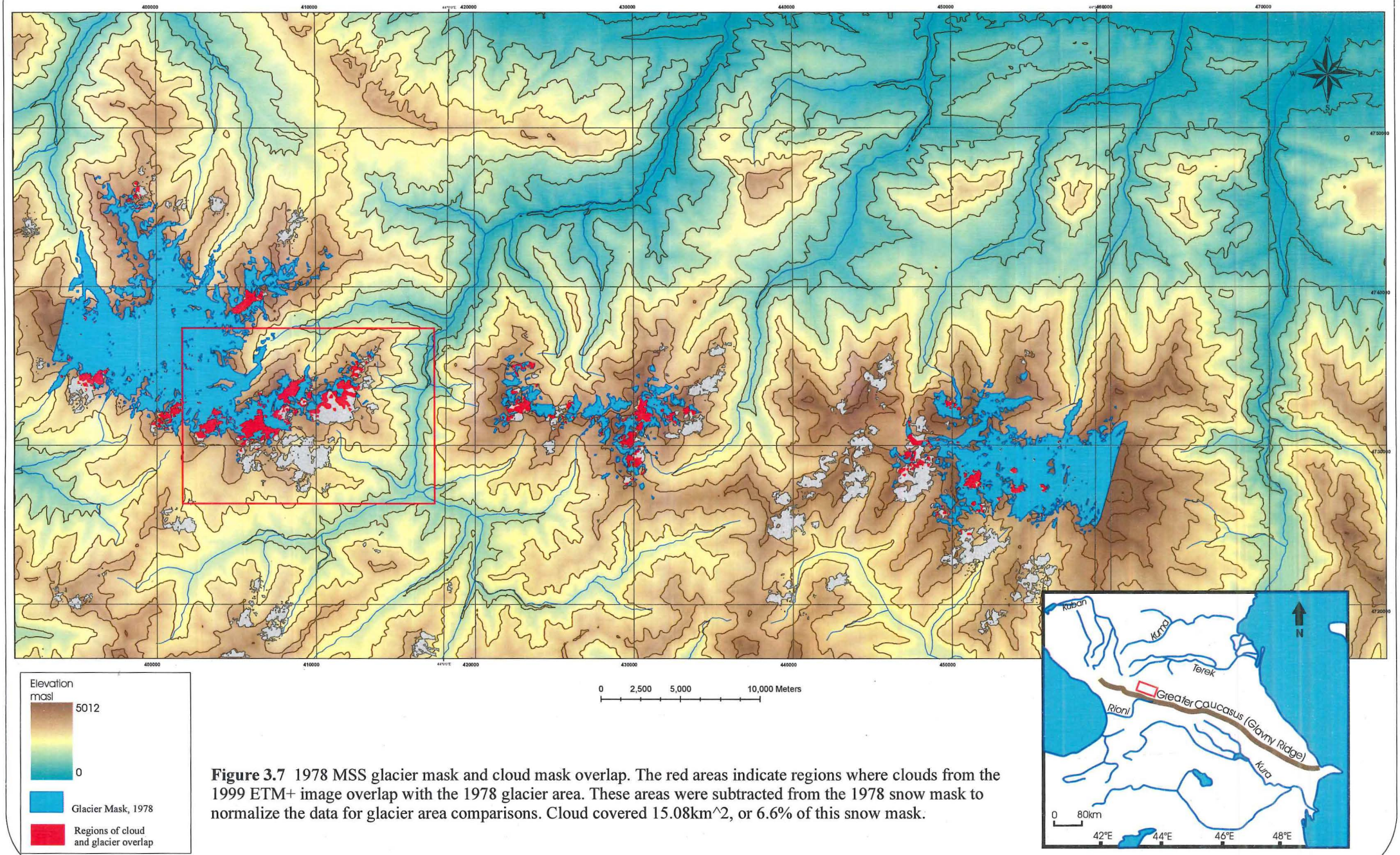

Figure 3.7 1978 MSS glacier mask and cloud mask overlap. The red areas indicate regions where clouds from the 1999 ETM+ image overlap with the 1978 glacier area. These areas were subtracted from the 1978 snow mask to normalize the data for glacier area comparisons. Cloud covered 15.08km^2, or 6.6% of this snow mask.

Snow and cloud have similar spectral signatures over the visible and near-IR parts of the electromagnetic spectrum, while divergence of their curves appears over the middle-IR. This divergence is the single most effective tool for distinguishing snow and cloud. The multispectral scanner operated in the visible and near-IR, but did not contain a channel for middle-IR radiation. Therefore, it is imperative that MSS images be acquired on completely cloud-free days for snow studies, as they lack the crucial spectral information that distinguishes snow from cloud. This is the only way to ensure that snow and cloud are not confused for each other.

The data that *is* contained in MSS spectral bands 1, 2, 3 and 4 are highly effective for vegetative studies (Landsat Data Sheet, accessed May 2007). Snow cover and other studies were, at the time of design, considered incidental or supplementary to vegetative and land-use studies. It was not apparent that cloud cover would severely impinge snow cover studies until after the launch and operation of the MSS.

Therefore, ultimately reducing the number of bands in the ETM+ image to correspond to the MSS image reproduced the shortcomings of the MSS data in the ETM+ data. It was decided that the results of this detection procedure would be discarded because of the loss of spectral information.

Snow Detection: Ratio Thresholding

The method that was the most successful at snow detection for the TM and ETM+ images was ratio thresholding. This technique takes full advantage of the spectral signature of snow over the middle infrared part of the spectrum. Few ground objects have such distinctly high reflectances in the near-IR and distinctly low reflectances in the mid-ID. This method is very similar to the snow index applied by Dozier (1987), but works faster and can be more easily adapted to the snow conditions in a particular scene (by adjusting the threshold values)

The ratio threshold images were preferred over the other techniques because the results were the cleanest and the technique was the most simple. It could be performed on many images quickly, while reducing the amount of incorrect classification that results from classifiers.

3.2.2 Areal Snow Extent Measurements

The following table summarizes the overall change between 1977 and 1999:

Image and date	Glacier extent (m^2)	Glacier extent (km^2)	Cloud covered area (km^2)	Difference from previous image (km^2)
MSS 25th Aug. 1978	189,593,890	189.59	15.08	0
TM 31st Aug. 1989	133,890,242	133.89	8.82	40.62
ETM+ 18th Aug 1999	114,916,656	114.92	?	10.15

Table 3.1 Changes in total glacier area detected by the glacier classification schemes described in the text.

The following table is the results of the calculated loss of glacier area for glaciers with terminus measurements, between 1971 and 1999:

Glacier Name	Glacier area change @ terminus 1971-1999 (km^2)
Kapaugom	0.351
Tseya	0.128
NW	0.000
NW1	0.050
NW2	0.056
NW3	0.026
NW4	0.007
NW5	0.029
SW1	0.070
SW2	0.129
Savitisi	0.051
MNA	0.016
Kolka/Maili	0.752
Total	1.665

Table 3.2 Glacier area change @ terminus for glaciers from which terminus position measurements were taken, 1971-1999

What is most striking about the results is the obvious reduction in glacier area between 1978 and 1999. The results are likely exaggerated for the years between 1978 and 1999, due to the different snow detection methods employed on the two different scenes, and also the differing ground resolutions. These results reflect loss of glacier ice from all areas, and are not exclusive of glacier retreat at the terminus. There has been a reduction in glacier area at places other than the terminus, including at nunatuks and lateral valley margins. In particular, there is a great reduction in the total area of glacier ice between 1978 and 1999 at places other than at the margins. Again, I point to this being the result of differing classification schemes and ground resolutions. Because the radiometric and spatial resolutions are similar in the TM and ETM+ images, I believe that this comparison is far more valuable (and accurate) than the one with the MSS image.

The total area of glacier retreat based on terminus measurements is significantly smaller than that measured with the snow detection methods, for two reasons. First, it measures only reduction in glacier area at the terminus. Secondly, it does not include measurements from all of the glaciers. However, because these measurements were taken manually and very carefully (I might add), they reflect an accurate representation of the loss of ice at the terminus.

3.2.3 Terminus Measurements

Terminus measurements were taken for 15 glaciers in the study area. The glaciers included in the study were selected based on how well they could be detected and their physical characteristics. Only glaciers whose terminus positions could be located with confidence were used. Table 3.3 summarizes the names, locations and retreat estimates for all of them.

Glaciers that could not be measured and the various reasons for it are summarized in Table 3.4. These glaciers were in most cases obstructed by clouds, but others were either partially or fully covered by debris.

Kapaugom Glacier

In the western part of my study area, the largest area of glacier ice is drained by the Kapaugom Glacier. It is the most significant glacier in the whole study area. The ablation zone feeds out north-northwestwards into a narrow valley. Several small glaciers feed it from the sides. On the eastern wall of the valley, there is a small glacier that does not feed into Kapaugom, but may have in the past during previous glacial advances. It would have contributed more ice to the Kapaugom main branch. Instead, it is likely that meltwater from this small glacier contributes to the thermal regime of Kapaugom locally on the east side.

Glacier Name	W/C/E	N/S	R/S/A	movement (m)	movement (m/yr)
Kapaugom	W	N	R	890	31.8
Tesya	W	N	R	335	12.0
NW1	W	N	R	0	0.0
NW2	W	N	R	230	8.2
Chalinginidete	W	N	R	235	8.4
Songutidontsete	W	N	R	175	6.3
NW3	W	N	R	70	2.5
NW4	W	N	R	215	7.7
SW1	W	S	R	330	11.8
SW2	W	S	R	235	8.4
Savitisi	E	S	R	530	18.9
MNA	E	S	R	520	18.6
Kolka/Maili	E	N	R	2150	76.8

W/C/E: west/central/east part of study area
N/S: north/south of Glaviny Ridge
R/S/A: retreat/stationary/advance

Table 3.3 Summary measurements for all glaciers with terminus position measurements.

Glacier Name	W/C/E	N/S	Reason for not being measured
Central Group	C	N	cloud cover
Midagrabin	E	N	cloud cover
Savitisi West	E	S	cloud cover
Kolka	E	N	debris cover/high levels of glacier activity related to physiographic environment
Maili	E	N	Kolka Glacier subsidiary arm
Chach	E	N	too far east
Devdoranskii	E	n/a	too far east/high level of mass wasting and glacier hazards
Abano	E	n/a	too far east/high level of mass wasting and glacier hazards
Ortsveri	E	S	too far east

W/C/E: west/central/east part of study area
N/S: north/south of Glaviny Ridge

Table 3.4 Summary of glaciers for which terminus measurements were not made, and the reasons for their exclusion from the analysis.

Terminus retreat is measured at between 830m and 890m, between Sept 20, 1971 and Aug 18, 1999 (Figure 3.7a and b). This glacier, together with Tseya, experiences a shift in glacial regime as a result of migration of the ice divide (see Section 1.2.5). The rate of retreat is the greatest measured, at over 31m/yr.

Tseya Glacier

Tseya Glacier jointly drains the western ice mass with Kapaugom Glacier (recall Figure 1.6). It is composed of two glacier branches. The ablation zone is heavily crevassed because of structural control exerted by the narrow valley.

Terminus retreat between Sept 20, 1971 and Aug 18, 1999 is roughly 335m (Figure 3.8a and b). At, 12.0m/yr, the rate of retreat is below average for the study area.

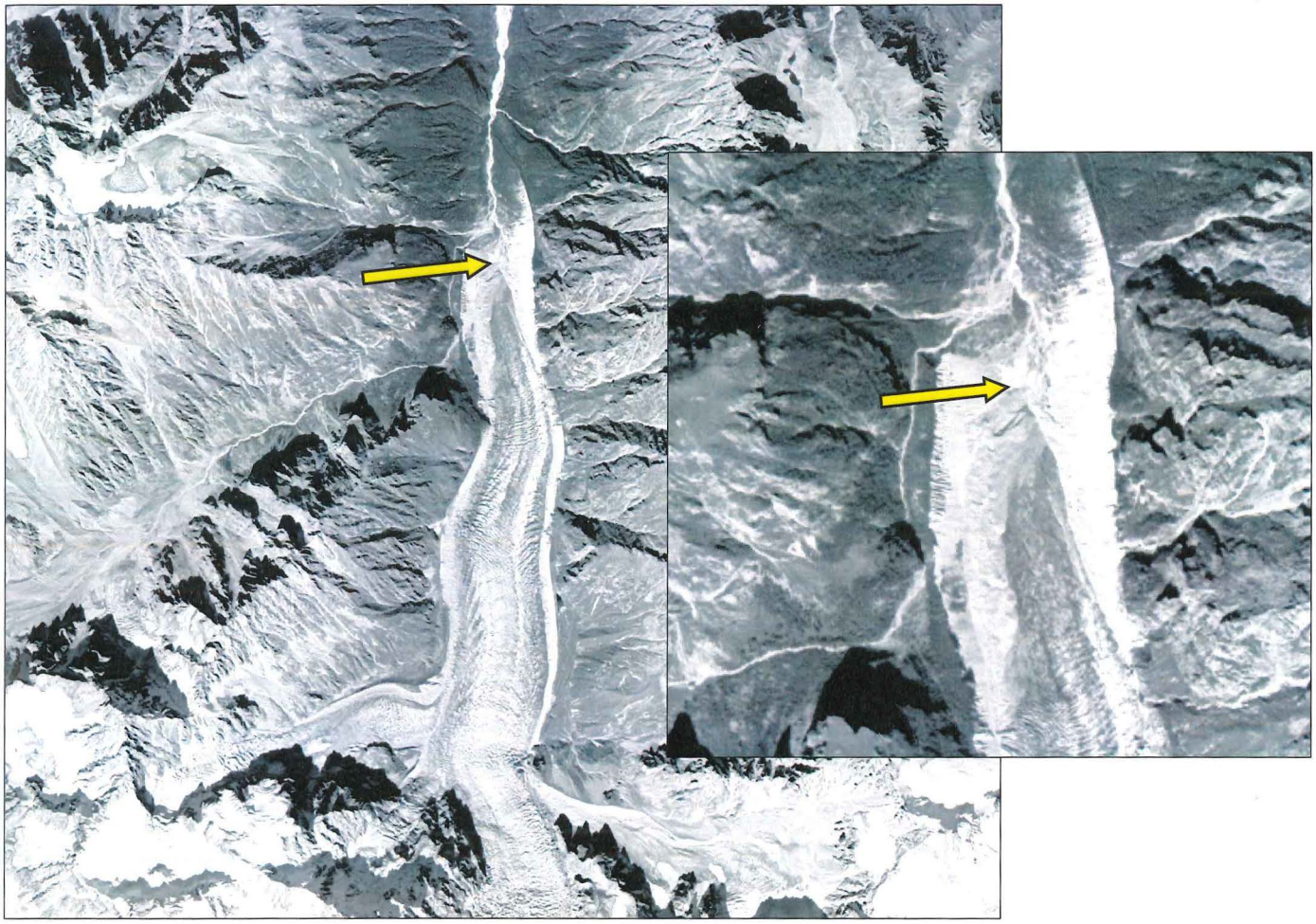

Figure 3.7a Kapaugom Glacier terminus position, 1971

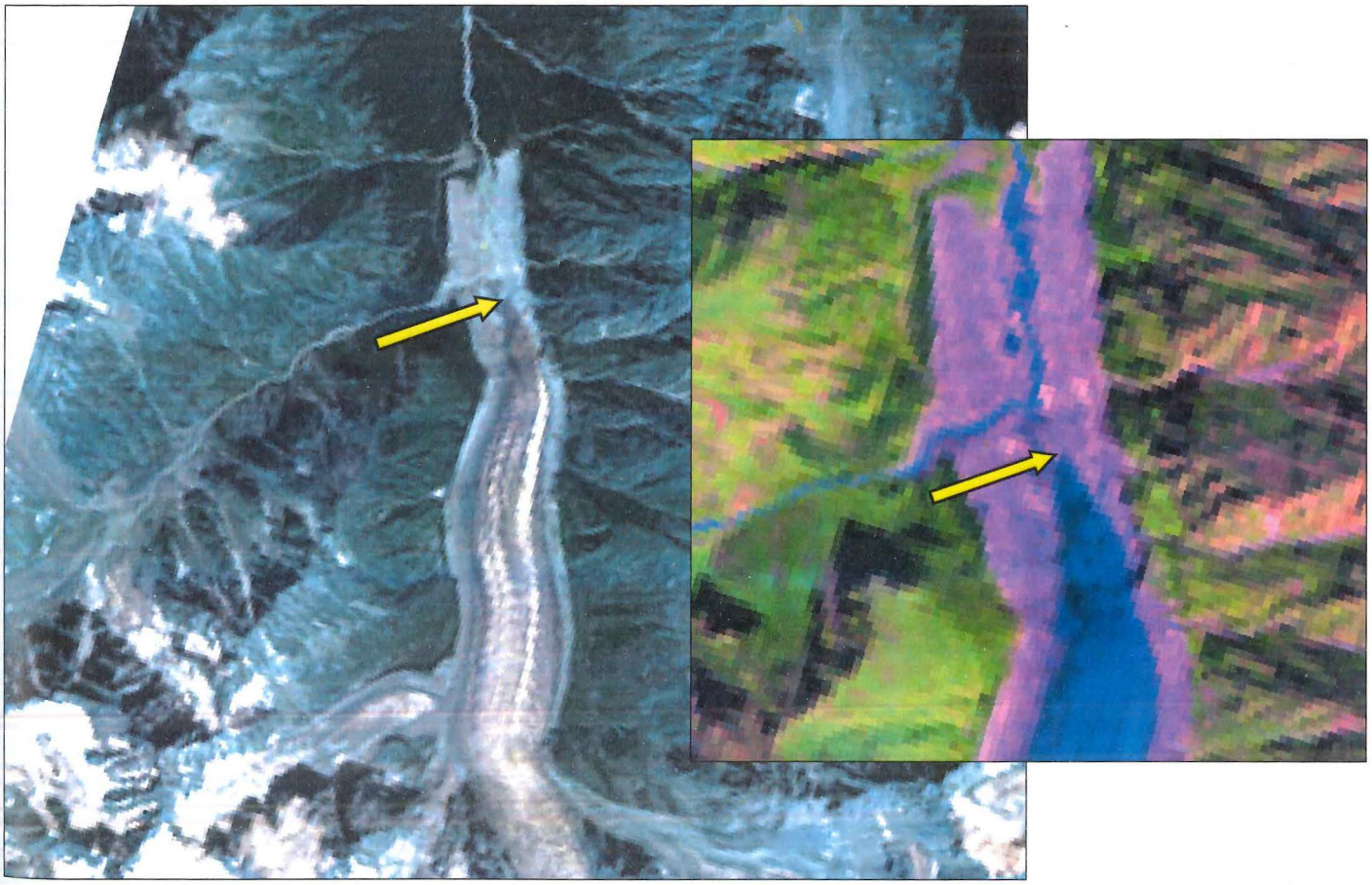

Figure 3.7b Kapaugom Glacier terminus position, 1999

Northwestern Glaciers

Chalinginidete, Songutidontsete, Donisartsete are a few of the glaciers that comprise a group of small northwestward-facing glaciers. These glaciers are not big; the 1999 Landsat image gives estimates on the order of a couple hundred square kilometres. Literature on these glaciers is absent, or at the very least inaccessible. It appears that they are among the glaciers whose behaviour is primarily a response to climate change, and are affected less by avalanching, surging, mass wasting and debris cover.

Terminus measurements were carried out for as many of this group as possible, and the results are summarized in Table 3.2. Measurements are significantly smaller than those observed at Kapaugom and Tseya, reflecting their small magnitude. Though retreat is less than at Kapaugom and Tseya, Chalinginidete Glacier retreated 235m, which is only 100m less than the retreat measured at Tseya. Terminus position change of NW1 glacier is negligible, while the other four glaciers retreated between about 70m (NW3 glacier) and 230m (NW2 glacier) (Figures 3.9a, b and 3.10a, b).

Retreat rates for this group are the lowest in the region, below 10m/yr for all measured.

Skazna and Zaramag Glaciers

Neither Skazna or Karamag Glaciers have detectable termini in the 1999 Landsat image.

Southwestern Group

Glaciers located in the southwest of the study area are much smaller than those on the north side, primarily as a function of aspect. Glacier size is roughly the same magnitude as those in the northwestern group, although retreat measurements are higher (Table 3.2). Retreat of SW1 is about 330m, though its areal retreat is only about 70,000m^2 because it drains into a narrow valley, while retreat of SW2 is about 100m less, but has an areal reduction of over 129,000m^2 (Figures 3.11a and b).

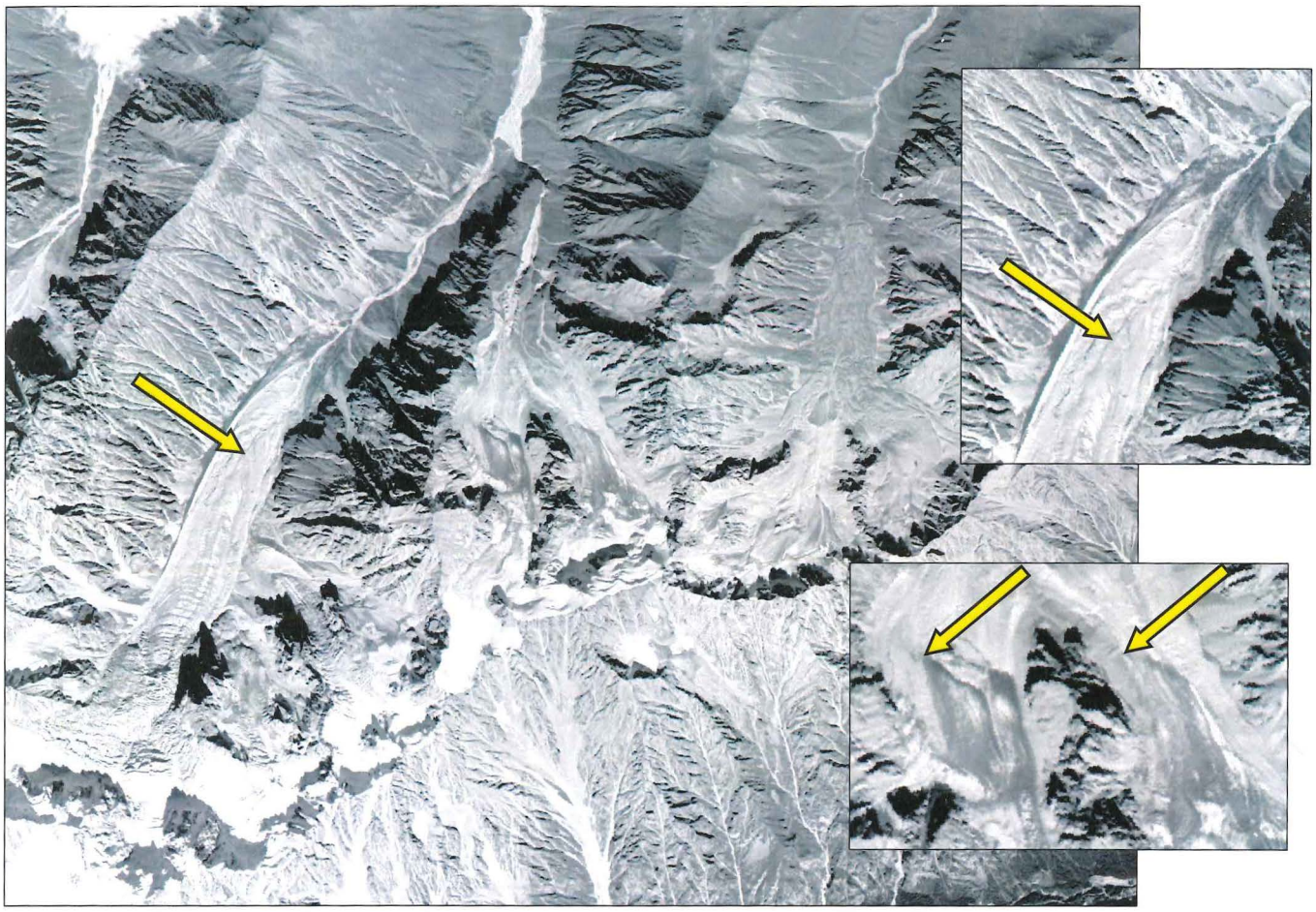

Figure 3.9a Northwestern Group of glaciers, terminus positions, 1971

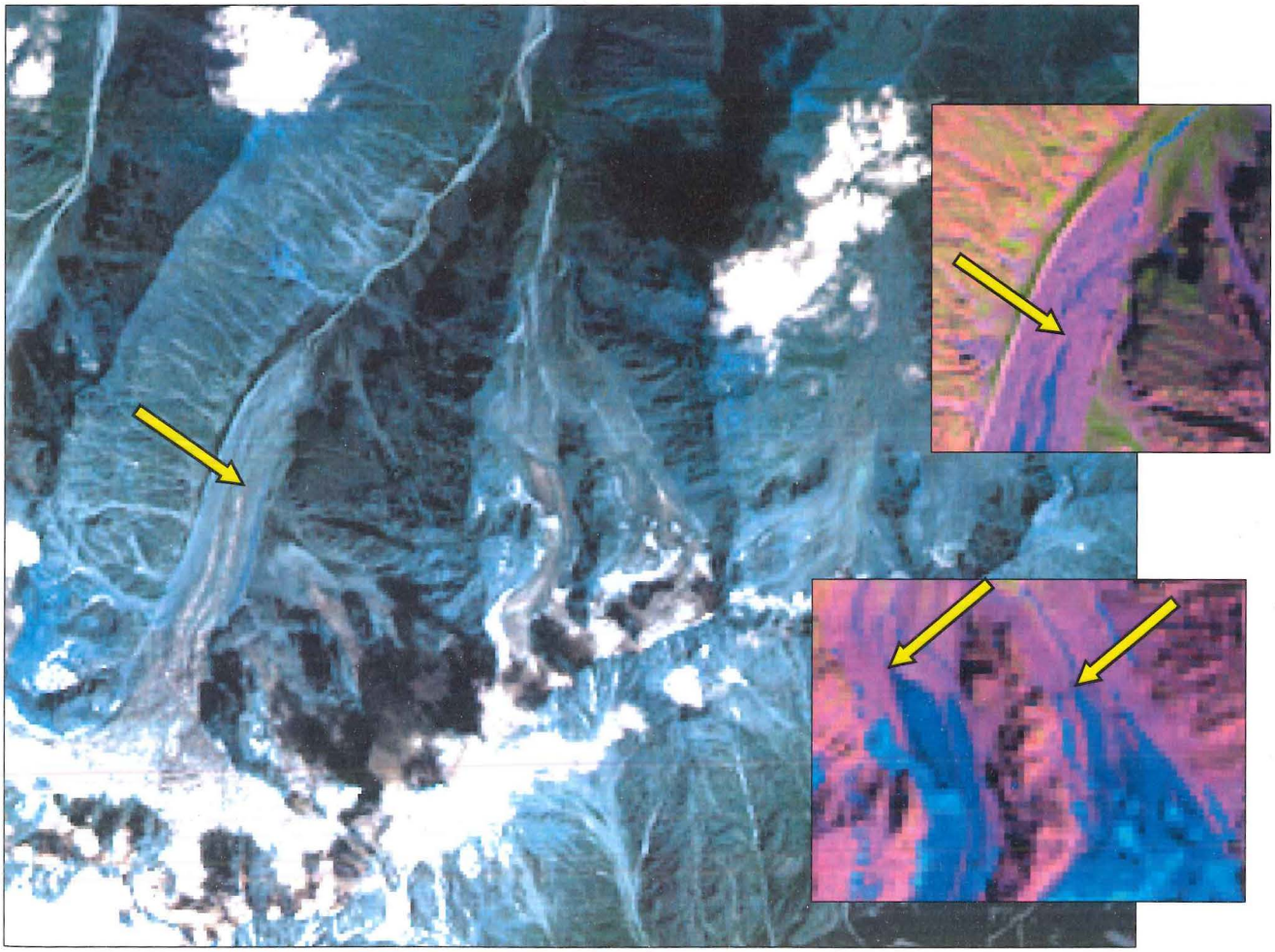

Figure 3.9b Northwestern Group of glaciers, terminus positions, 1999

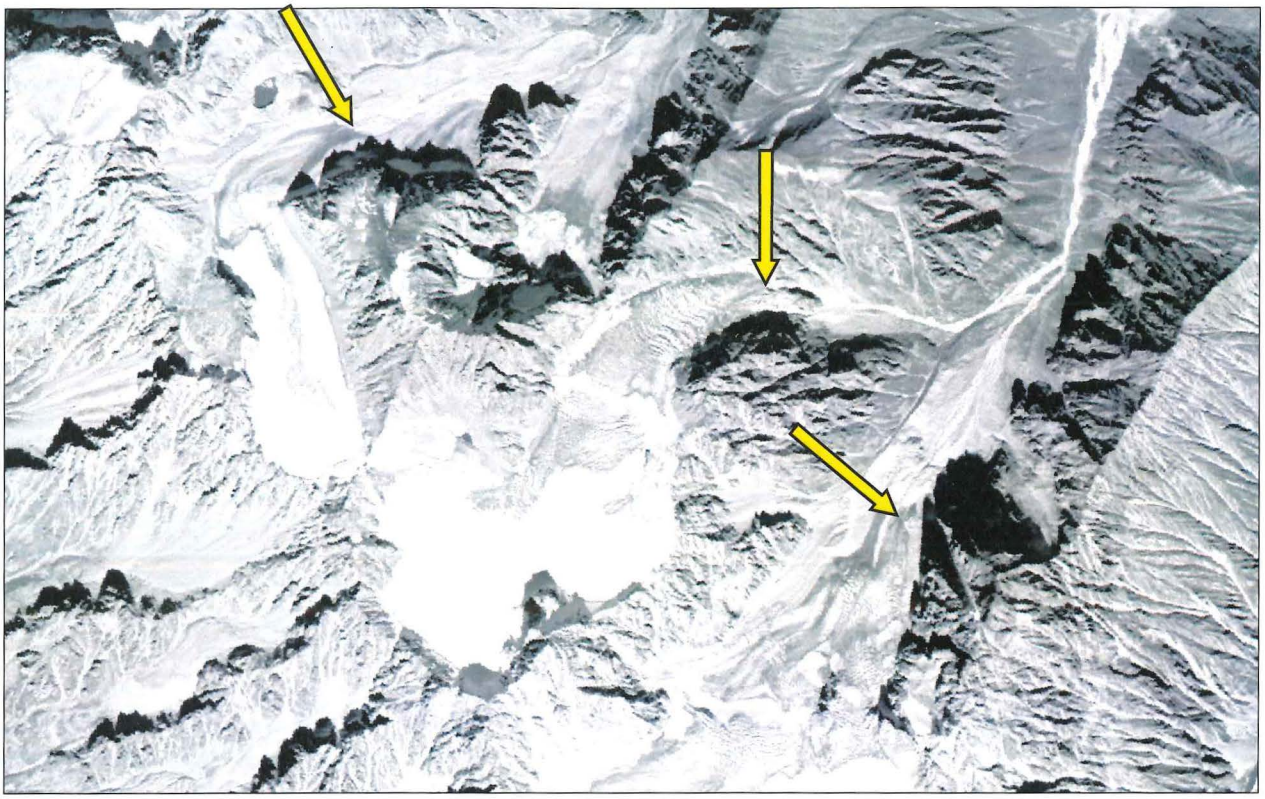

Figure 3.10a Northwestern Group of glaciers, terminus positions, 1971

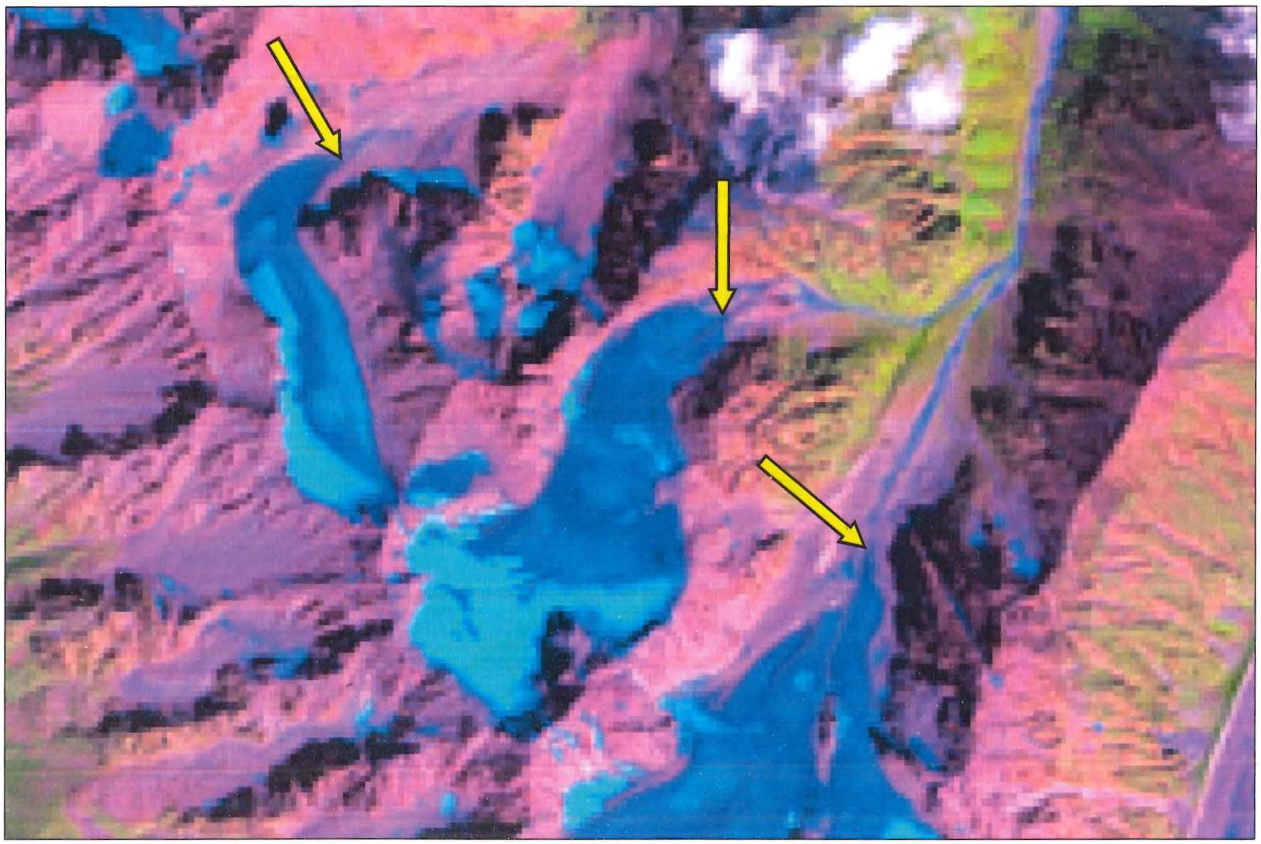

Figure 3.10b Northwestern Group of glaciers, terminus positions, 1971

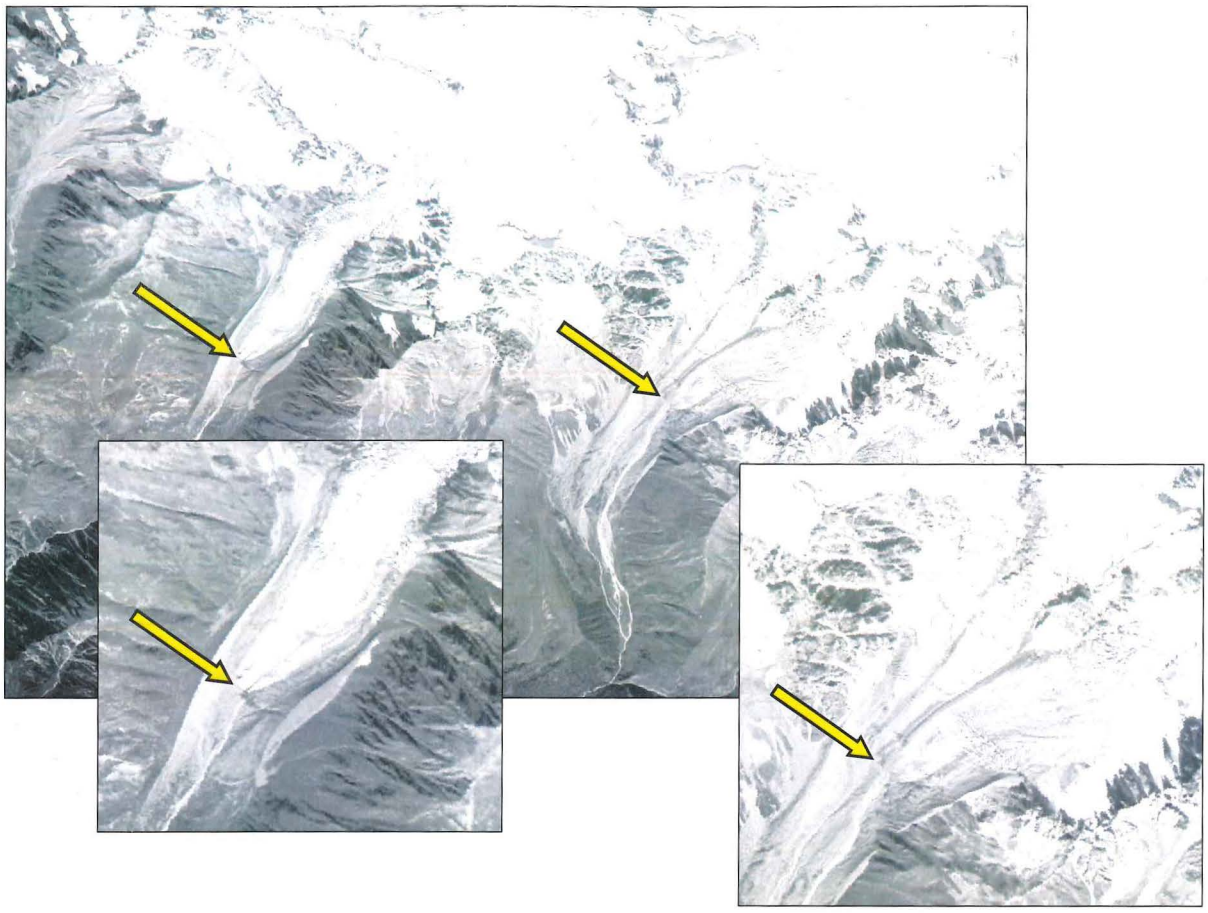

Figure 11a Southwestern Group of glaciers, terminus position measurements, 1971

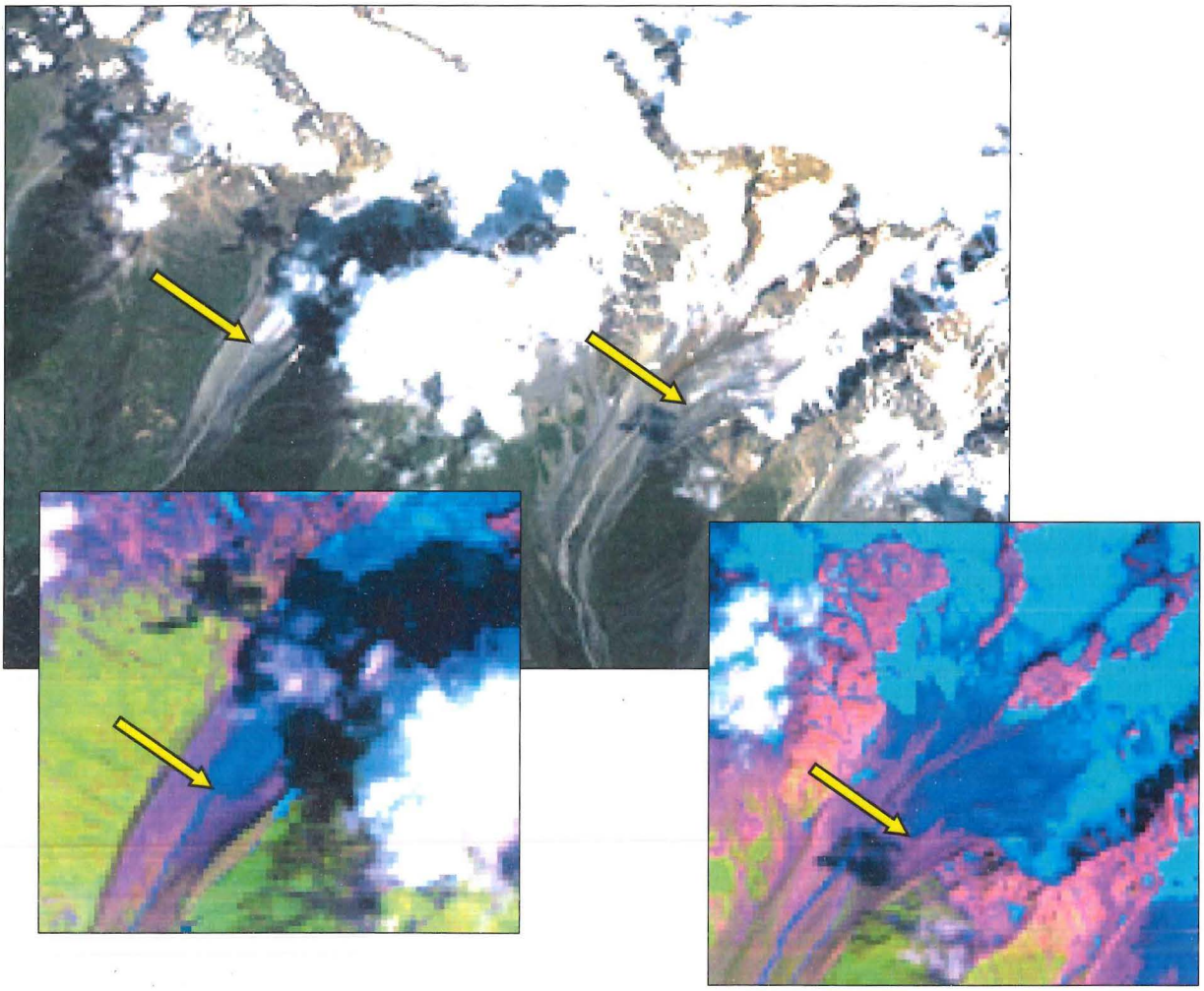

Figure 11b Southwestern Group of glaciers, terminus position measurements, 1999

Central Glaciers

There is a group of very small glaciers and permanent ice patches located in the centre of the study area. Measurements were not carried out here because of cloud cover.

Midagrabin Glacier

Perched alone on the western flank of Mt. Kazbek, Midagrabin has typical morphology for the area with its steep headwalls and narrow valley outlet. However, unlike many of the other glaciers descending from the slopes of Kazbek, there is very little debris at the surface. There is also no known past hazardous activity. Unfortunately, once again, this glacier's terminus is not visible in the 1999 Landsat image because of cloud cover and therefore was not investigated.

Kolka and Maili Glaciers

Completely buried beneath a debris cake, Kolka is one of many glaciers on Kazbek that behave extremely erratically. Not only is the terminus totally obscured (thereby precluding even the possibility of even finding the terminus), but also measurements made here would be in vain, due to surging events and glacier disasters. The position of Maili Glacier's terminus is dependent on the location of Kolka because during Kolka advances, it is cut off and both feed into the main valley simultaneously. In the past, Maili was given credit for the glacier disasters that were probably occurring on Kolka (Heybrock, 1935). Maili probably behaves quite regularly, even if it is a feeder glacier for Kolka during periods of glacial advance. Interestingly, however, the extent of these two glaciers in 1971 was *vastly* greater than in 1999 (Figures 3.12a and b). The reduction in glacier area is the highest in the region, at about 750,000m^2, and well over 2km in length. No records for violent glacial events were found to have occurred within that time frame.

Savitisi and MNA Glaciers

Savitisi and MNA are both located on the south side of Mt. Kazbek, but are remain a part of the Terek River watershed. It is characteristic of the southern side of the Caucasus to have glaciers of far lesser length, but greater width than the northern side. This reflects the mountain physiography in that valleys become significantly narrower lower down in the mountains. Savitisi and MNA terminate at around 3300m and do not infiltrate the valleys below. MNA is included in the glacier terminus measurements from the WGMS, though data were not available for comparison with the results of this study. Terminus fluctuations are lesser than those on Kapaugom the west, but greater than all other glaciers in the study at 530m and 520m, respectively (Table 3.2 and Figures 3.13a and b).

Chach, Devdorak, Abano and Ortsveri Glaciers

The Landsat 1999 image did not capture these glaciers. However, erratic behaviour at Devdorak and Abano make them unsuitable for measurement.

3.2.4 Climate Trend Analysis, Caucasus

Table 3.5 summarizes the results of the climate trend analysis for the variables precipitation and temperature. There are no time-series over the period of 1971-1999 that indicate any trend, positive or negative, for either climate variable.

Glacier fluctuations in the Caucasus are best described by a combination of precipitation and temperature data. Recall that the Caucasus has an intermediate glacial regime between continental and maritime end-members. Winter precipitation trends are a slightly better approximation of accumulation trends than annual precipitation, as winter temperatures are normally sub-zero and so produce snowfall. Similarly, summer temperatures are a better index than annual temperatures for annual ablation because they are normally positive and therefore indicate times during which there is surplus for glacial melting (Benn and Evans, 1998).

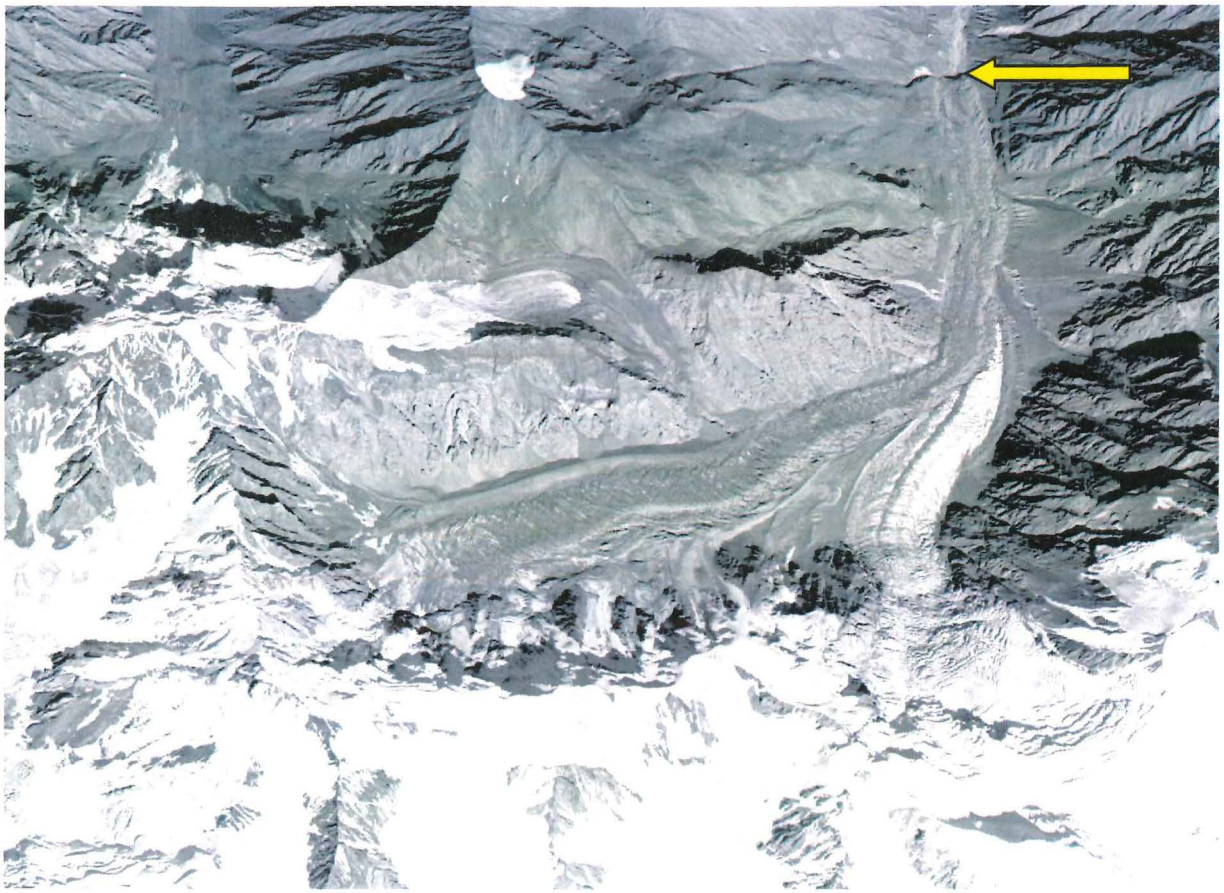

Figure 3.12a Kolka and Mailik Glaciers, terminus position,1971

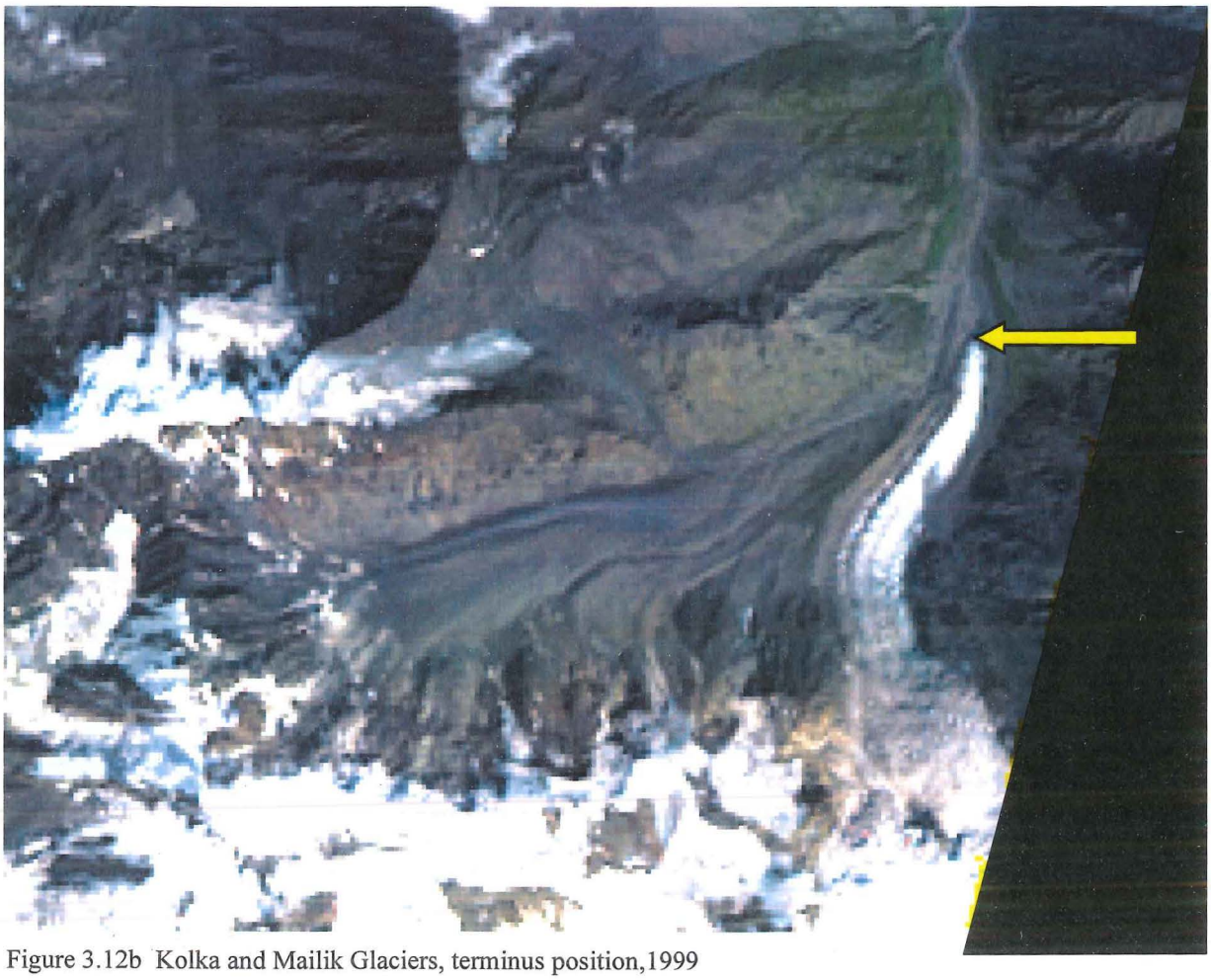

Figure 3.12b Kolka and Mailik Glaciers, terminus position,1999

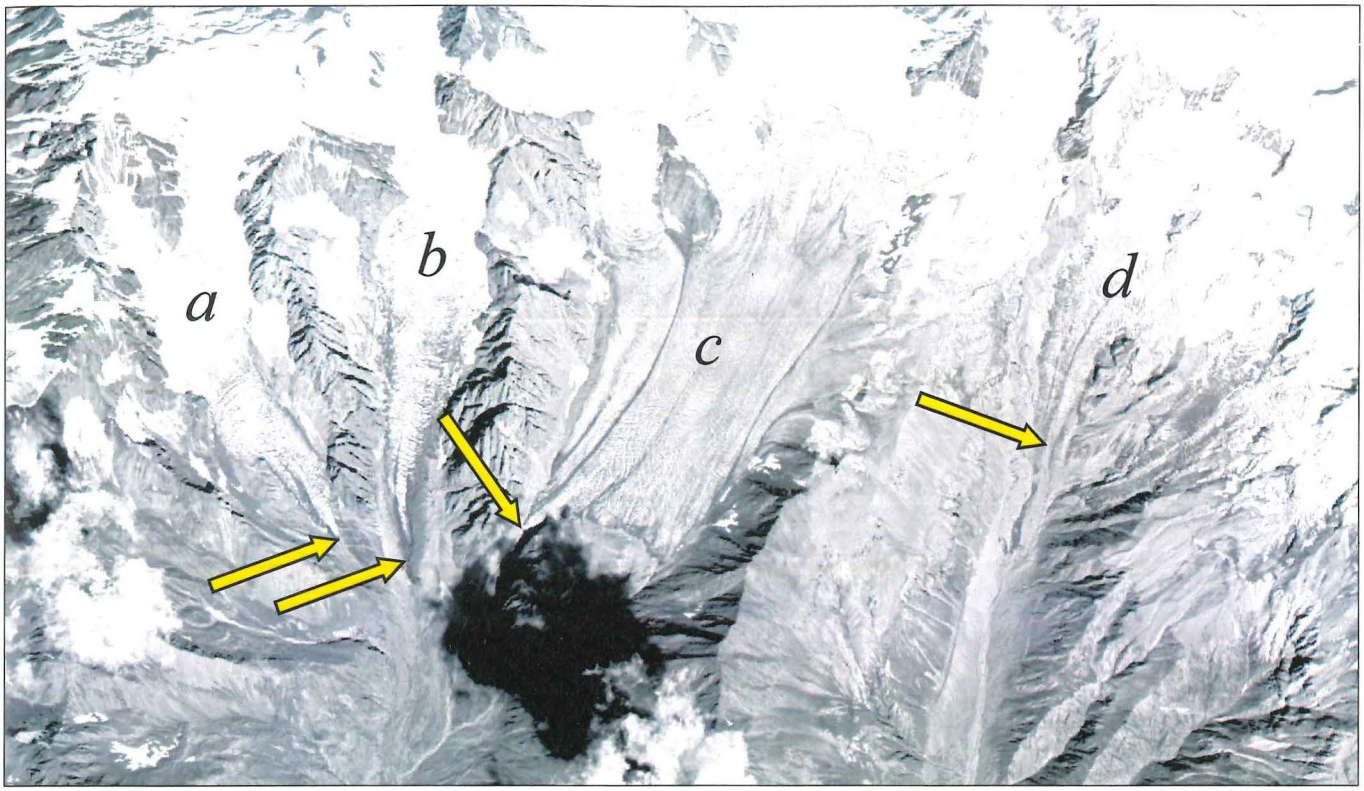

Figure 3.13a Savitisi and MNAglacier termini positions, 1971. Locations a (a) and (b) are the west branch of Savitisi Location (c) is the main branch and (d) is MNA glacier

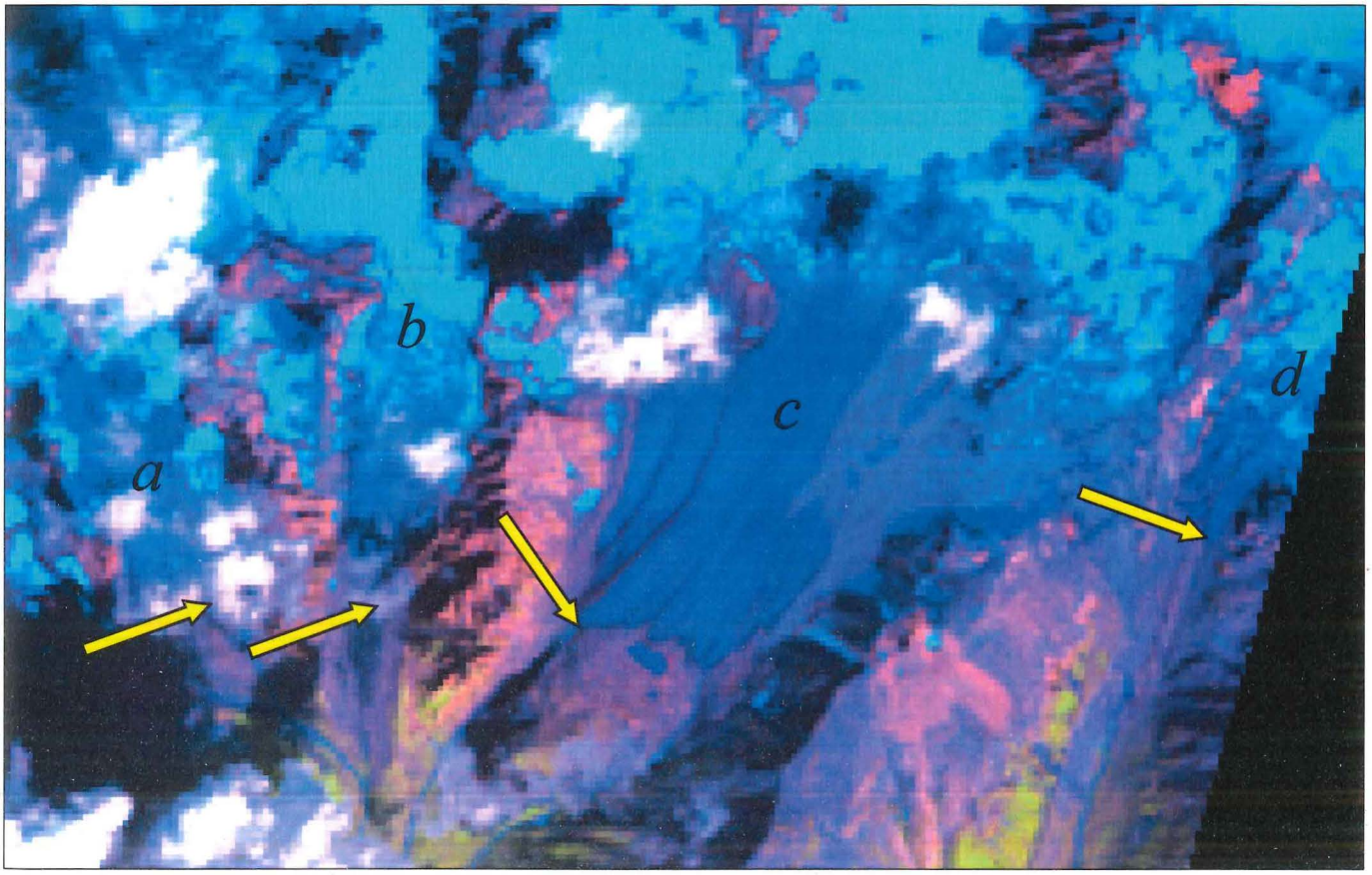

Figure 3.13b Savitisi and MNAglacier termini positions, 1999. Locations a (a) and (b) are the west branch of Savitisi, obscured by cloud. Location (c) is the main branch and (d) is MNA glacier

Precipitation figures show high interannual variability (Table 3.5 and Figure 3.14) between 1971 and 1999, while no time-series during that time show a linear trend (significant at 0.05, or any level). From the graph, it's obvious that summer precipitation comprises most of the precipitation in a year. Winter and summer precipitation do not share the same pattern from year to year, suggesting that both interannual and intra-annual variability is high.

Grid cell beginning 44°00'E, 42°30'N				
	Precipitation		Temperature	
	annual	winter	annual	summer
r-sq	0.0168	0.0124	0.0104	0.0232
N	29	29	29	29
t	0.685006	0.585884	0.535475	0.810252
p	0.249589	0.28141	0.298353	0.21244
Grid cell beginning 43°30'E, 42°30'N				
	Precipitation		Temperature	
	annual	winter	annual	summer
r-sq	0.0179	0.0069	0.0193	0.0007
N	29	29	29	29
t	0.707869	0.434624	0.736079	0.137574
p	0.242547	0.333645	0.234015	0.445799
Grid cell beginning 43°00'E, 42°30'N				
	Precipitation		Temperature	
	annual	winter	annual	summer
r-sq	0.0197	0.0028	0.0158	0.0001
N	29	29	29	29
t	0.743971	0.275727	0.663632	0.051967
p	0.23166	0.392429	0.256277	0.479469

Table 3.5 Caucasus trend analysis summary data. No time-series reflects a trend significant at 0.05, or any level.

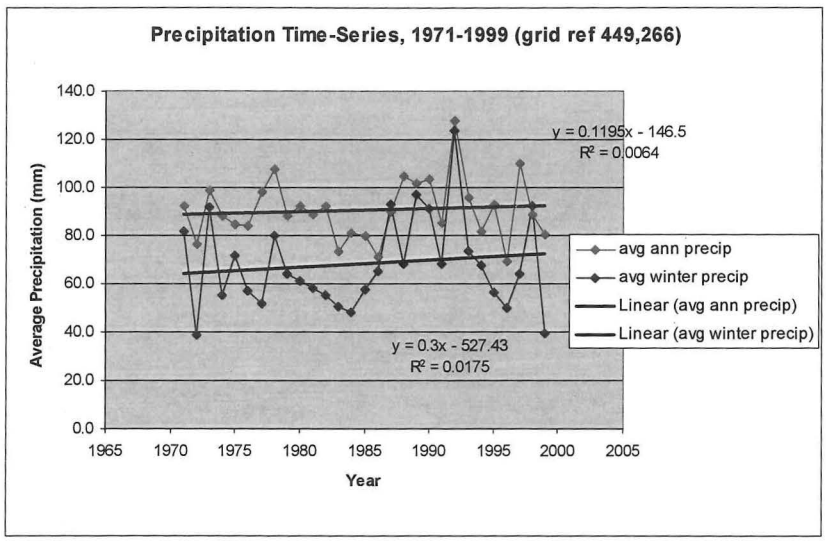

Figure 3.14 Precipitation Time-Series, 1971-1999. CRU grid cell beginning 44°00'E, 42°30'N.

Temperature data exhibits low variability about the mean for both summer and winter temperatures, but does not exhibit a linear trend (significant at 0.05) (Table 3.5). Summer temperatures tend to show less variability than annual temperatures, especially from 1980 onward. Annual temperatures calculated over the entire period have maintained a sub-zero average (-0.2°C). There are only 8 years in the time-series (Table 3.6) that have an above-freezing average temperature. Besides those years, all years have seen sub-zero average annual temperatures (Figure 3.15). Average summer temperature hit a high in 1975 (11°C) and has not reached that level since. The last four years of the summer time series have not been notable in any way, except to note that they vary very little about the 29-year mean.

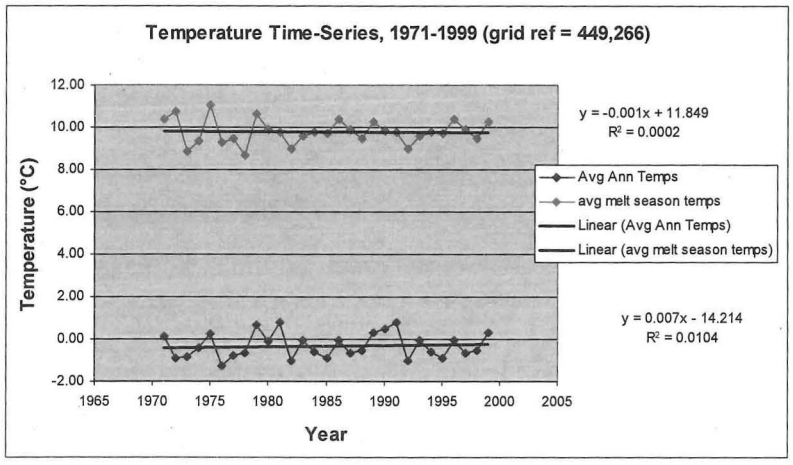

Figure 3.15 Temperature Time-Series, 1971-1999. CRU grid cell beginning 44°00'E, 42°30'N.

Year	Average Temp. (°C)
1971	0.11
1972	-0.91
1973	-0.87
1974	-0.43
1975	0.23
1976	-1.27
1977	-0.76
1978	-0.67
1979	0.65
1980	-0.11
1981	0.79
1982	-1.01
1983	-0.06
1984	-0.62
1985	-0.88
1986	-0.07
1987	-0.67
1988	-0.53
1989	0.28
1990	0.49
1991	0.79
1992	-1.01
1993	-0.06
1994	-0.62
1995	-0.88
1996	-0.07
1997	-0.67
1998	-0.53
1999	0.28

Table 3.6 Average annual temperature 1971-1999

3.2.5 Comparative Trend Analysis

The results of analysis for the Alps are presented in Table 3.7. The overall annual trend indicates a warming signal coming from temperature, without compensation in the amount of annual precipitation. Analysis for winter precipitation (snow) and summer temperature shows a similar pattern.

In the early half of the 20th century, it was widely regarded that Caucasus glaciers and Alpine glaciers exhibited the same or remarkably similar patterns in terms of growth and decay (Horvath and Field, 1975). The net balance of these two areas was suggested to mimic each other in the same cycles. Upon investigation, it was found that the behaviour of Alpine and Caucasus glaciers over the last half of the 20th century, and especially over the study period (1971-1999), have taken a distinct departure from each other. This prompted correlation analyses for each region to assess differences in climatic regime. It is hypothesized that differences in climatic variable trends can be used to explain the difference in glacier behaviour in glaciated areas worldwide. In particular, it is thought that differences in winter precipitation and summer temperature trends in the Alps and Caucasus can help explain differences in observed glacier behaviour.

Grid cell beginning 07°00'E, 45°30'N				
	Precipitation		Temperature	
	annual	winter	annual	summer
r-sq	0.1542	0.2678	0.2683	0.2512
N	29	29	29	29
t	2.412439	3.672463	3.678402	3.47797
p	0.011456	0.000523	0.000515	0.000864

Table 3.7 Alpine trend analysis summary data. All data are significant at at least 0.05, and most at 0.01

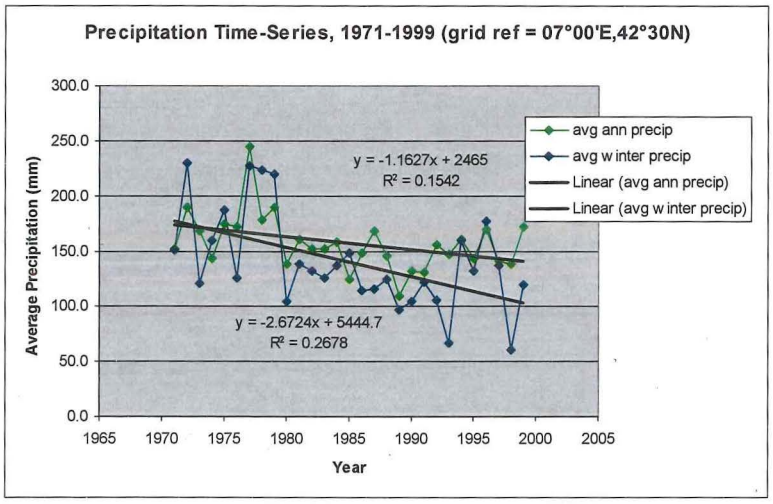

Figure 3.16 Alpine Precipitation Time-Series, 1971-1999. CRU grid cell beginning 07°00'E, 42°30'N.

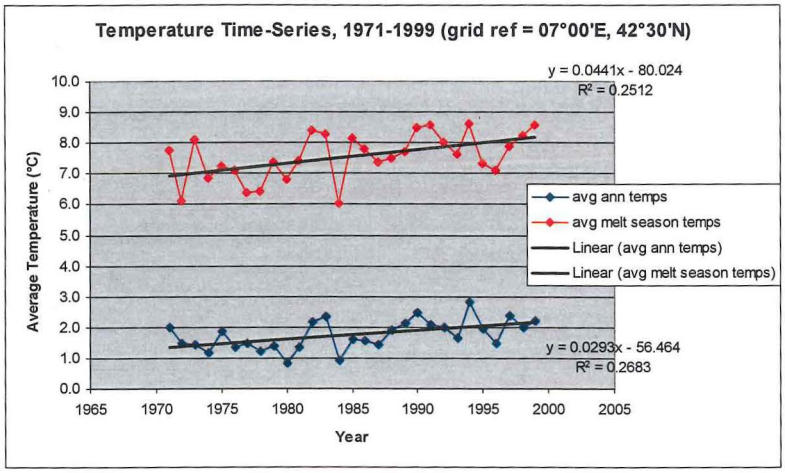

Figure 3.17 Alpine Temperature Time-Series, 1971-1999. CRU grid cell beginning 07°00'E, 42°30'N.

These data clearly show a significant (at 0.01) warming signal from the Alps, without a compensating increase in the level of annual precipitation. The opposite is observed: the trend in precipitation is negative, amplifying the effect of warming temperatures on glaciers. The mass balance regime for Alpine glaciers has been increasingly negative since the start of the rise of global temperatures in the 1860s. The data in Table 3.8 highlights the negative trend observed in the Alps relative to other glaciated regions.

CHAPTER 4

DISCUSSION

4.1 REMOTELY SENSED DATA AND THIS GLACIER STUDY

There are a few things to note about image acquisition and preparation. The only way to appreciate how important it is that images are compatible with each other in environmental monitoring and analysis is to experience the process. For the analysis conducted here, the datasets were not compatible with each other in a myriad of ways. Necessary steps were taken to overcome the incompatibility, but were not always as successful or as easy as one would hope. Understanding how important and time-consuming this process is only really happens after the process is complete.

[1] Orthorectification of images taken over mountainous regions is absolutely crucial for fast, streamlined change detection. Although qualitative analysis is possible without orthoimages, quantitative analysis is either very difficult or impossible. During measurement of terminus positions this became painfully apparent. Termini could be quantitiatively measured in places where the bed slope was negligible; otherwise geometric distortions would introduce errors into the measurements. Fortunately, Caucasus glaciers have shallow beds and so such measurements were possible. Unfortunately, lack of orthorectification required that at least two ground control points be identified in each image in order to calibrate measurements every single time one was taken. This process could have been avoided if the photographs were geometrically corrected beforehand.

Another problem concerning terrain normalization arose with the Landsat ETM+ image. The L1G Landsat images are nominally ready-to-use, however; because they are not geodetically compatible with NASA GeoCover images, there were undesirable offsets among them that may have led to misinterpretation of the results. To perform automated measurements and techniques, geodetic compatibility is necessary. Image overlay is simple, but is a type of analysis that requires geodetic agreement among all images. For example, the results presented in Map 1 show glacier extent in 1978, 1989 and 1999 overlaid for direct comparison. The snow masks could be used to speculate about the observed spatial differences in terms of lateral glacier movement, but lateral differences

in the snow masks are likely the result of georeferencing errors. Therefore it would be very difficult to draw conclusions about glacier width changes with respect to the valley walls.

[2] Cloud covered areas were effectively removed from the study area. To emphasize again on the importance of georeferencing, one of the techniques that eliminated most of the cloud cover (PCA), relied heavily on adequate compatibility between images. For single-image studies, the presence of bands 5 and 7 on the ETM+ is invaluable for cloud detection. These bands improve differentiation between clouds and other ground objects.

4.2 Glacier Behaviour and Climate Analysis

The following statements can be made regarding the observed glacier behaviour and climate analysis results in the Central Caucasus Mountains of Russia.

[3] Of the 15 glaciers involved in the study on terminus position measurements, all but one had exhibited to a greater or lesser degree, a retreat of the terminus position from its 1971 condition. Glacier area analysis also shows an overall reduction in glacier ice from 1971-1999, 1978-1999 and 1989-1999. This observed behaviour suggests a warming signal from the Caucasus region. But, to what degree is such warming occuring? Climate statistics do not show a warming trend significant at a confidence level of 0.05%. Although this threshold is arbitrary, many other glaciated regions show a warming trend at least that significant, while the Caucasus exhibits high interannual climatic variability and virtually no trend at all. When climate variables are reorganized to highlight summer temperatures – again – a warming trend is not evident. Therefore *it is not possible to conclude*, based strictly on the CRU climate data, that a warming trend during the years 1971-1999 produced the observed glacier behaviour.

However, it is possible that other indicators can provide additional clues to facilitate more concrete statements about climate trends and glacier behaviour.

[4] It is useful to attempt the analysis in reverse, by using glacier variables as indicators of prevailing climate trends. This is in addition to what has already been done in the study; i.e. using climate variables as an explanation for observed glacier behaviour. We have seen that mountain glaciers are highly sensitive indicators of climatic change, responding in short-term to the annual temperature cycle and precipitation regime. This annual climatic cycle controls the annual mass balance response for a given glacier, while the long-term climate regulates the accumulated mass balance responses. At this juncture, I want to reintroduce the available mass balance data for Djankuat Glacier to give further insight into the prevailing climate. This will allow more concrete conclusions about the link between glacier retreat and the climate warming that has been indicated in the trend analysis.

Both the summer and winter balance data are measured at Djankuat. Mass balance data for Djankuat by time-series are presented in Figure 4.0 and Table 4.0 (data from Dyurgerov, 2002). The net mass balance is divided into components: specific winter mass balance (b_w) and specific summer mass balance (b_s). The annual net balance is defined $b_w + b_s = b_n$, where b_s is a negative value.

Table 4.1 highlights years where the net mass balance was either positive or negative. Between 1971 and 1999 the pattern is obvious: there is high interannual variability, with years of positive and negative mass balance frequently alternating. Net mass balance components likewise show high variability between years. Within the accumulation and ablation data, there is no time-series that suggests a trend significant at 0.05 (Shahgedanova 2005).

The cumulative mass balance hit a significant low in the 1985-86 mass balance year, indicating that the overall trend may have been a general decrease in glacier mass (and therefore extent and volume). While years of negative balance have occurred consecutively on four occasions between 1971 and 1999, there has been only one time that consecutive positive years have occurred. However, substantial amounts of snowfall during years of positive mass balance have helped sustain glacier mass during this period.

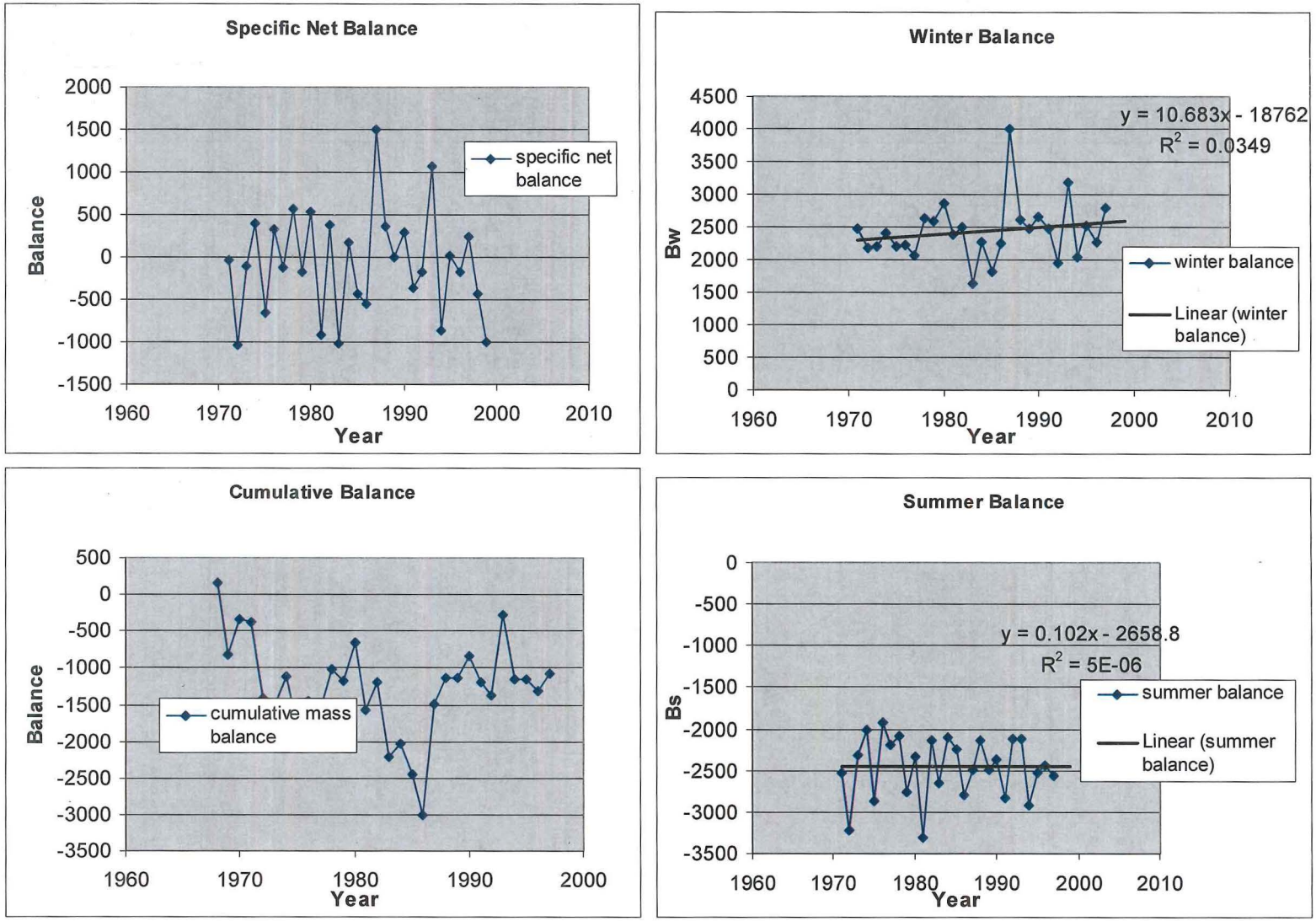

Figures 4.0a through b Djankuat Glacier balance regime, 1971-1999 (units in cm) (a) Djankuat Glacier specific net balance (b_n), 1971-1999 (b) Cumulative mass balance (b_c) (c) Winter balance (b_w) and (d) Summer balance (b_s)

Year	bn	bw	bs	bc
1967				
1968	154	2042	-1877	154
1969	-977	1879	-2855	-823
1970	486	2406	-1920	-337
1971	-40	2486	-2527	-377
1972	-1032	2182	-3214	-1409
1973	-107	2201	-2308	-1516
1974	397	2403	-2006	-1119
1975	-652	2211	-2864	-1771
1976	327	2237	-1910	-1444
1977	-129	2064	-2193	-1573
1978	561	2636	-2075	-1012
1979	-167	2584	-2752	-1179
1980	531	2857	-2327	-648
1981	-914	2385	-3299	-1562
1982	372	2508	-2136	-1190
1983	-1014	1637	-2651	-2204
1984	173	2264	-2091	-2031
1985	-423	1809	-2231	-2454
1986	-545	2243	-2788	-2999
1987	1507	4003	-2496	-1492
1988	369	2616	-2131	-1123
1989	-8	2479	-2487	-1131
1990	298	2658	-2360	-833
1991	-358	2468	-2826	-1191
1992	-171	1951	-2122	-1362
1993	1077	3183	-2106	-285
1994	-867	2048	-2915	-1152
1995	10	2530	-2520	-1142
1996	-172	2262	-2434	-1314
1997	240	2797	-2557	-1074
1998	-430			-1504
1999	-1000			-2504

Table 4.0 Tabular time-series balance regime data for Djankuat Glacier. b_n = net balance, b_w = winter balance, b_s = summer balance and b_c = cumulative mass balance.

The mass balance data suggests support for the idea that between 1971 and 1999 there was very little climatic variability in the Caucasus, and that led to only minor glacier fluctuations. The observations of glaciers that have responded primarily to climate change over this time may reflect a longer-term climate signal than that of the 28 years between 1971 and 1999

[5] Glaciers of small area and volume have the highest mass turnover rates, as their small mass is easily replaced by heavy snowfall and high summer temperatures. The mass balance of very small glaciers and perennial snow patches fluctuates from

year-to-year much more than that of large glaciers, thereby reflecting interannual climate variability (Dyurgerov, 2002; Glazyrin et al, 1993; Kuhn, 1995). These glaciers are very sensitive, short-term climate indicators. The group including Chalinginidete, Songutidontsete and Donisartsete Glaciers represent this type. Terminus fluctuations among this group are not large between 1971 and 1999, suggesting that they reflect the unchanging climate during this period. Larger glaciers, like Kapaugom Glacier, register greater losses, which again, may reflect climate trends of a greater order of magnitude.

[6] South-facing glaciers register high losses over the study period, which may have more to do with their physiography than the climate. These glaciers are exposed to winter and summer air masses from the subtropical south, which can be significantly different from the air masses on the north side of the range. It is possible that the CRU average temperature data for grid cells over the Caucasus are influenced to a greater degree by weather stations to the north, in Russia. Moreover, these glaciers are exposed to more solar radiation than those on the north, which provides additional energy for melting ice.

Comparisons

[7] Compared to Alpine glaciers, there is *remarkably* less glacier retreat in the Caucasus. The Alps have a very strong warming trend (significant at 0.01), with no compensating trend in winter precipitation levels. This relative difference may be attributed to two things: differences in glacier physiography and climate circulation patterns. The general circulation pattern of the Caucasus may differ significantly from that of other glaciated areas like the Alps, though there is little evidence to prove this or otherwise. More work in this area may be warranted.

[8] Of the glaciers included in the study of areal ice extent, several have regimes that make them 'special cases.' From the earlier discussion of physiography, it is clear that this study area contains an array of different glacier regimes/types. It is important to know which glaciers behave in ways contrary to the regular behaviour exhibited by glaciers in response to climate change. We have seen that some of them were difficult to detect by satellite measurements without explicit knowledge of their existence. These are intensely debris-covered glaciers. They are so intensely layered with

surficial material in fact, that even after prolonged work with the Landsat images, the spectral and spatial resolution proved too coarse to make any type of measurements on them. Kolka glacier and Donisartsete are both examples of this type. For this reason, they were not included in the study of terminus fluctuations.

For interest's sake, the co-terminus of Mailik and Kolka Glaciers was measured. This terminus appears to have had the greatest retreat of any in the region, probably as a result of the physiographic forces described in this paper, such as glacier hazards and severe mass wasting events. Climate variables are unlikely to give any reasonable indication of the behaviour of Kolka and Mailik glaciers. Similarly, Dedorak and Abano Glaciers on the east side of Mt. Kazbek were not included in the study due to the erratic, disastrous nature of the events that take place on them.

CHAPTER 5

CONCLUSIONS

FINDINGS

Remote sensing is a valuable tool to use in glaciological studies. The remote and hazardous nature of glaciated environments lends easily to remote assessment. Glacier behaviour and events which occur at times when humans are not present can be observed and documented. This includes all forms of high mountain hazards and glacier behaviour.

Image compatibility streamlines the process of analysis with remotely sensed images, creating an environment where qualitative analyses are less labour intensive. However, the process of creating this environment is not necessarily an easy one, though tools exist to make it possible.

The Central Caucasus defines a region where remotely sensed imagery has great value and applicability. As a hazardous environment with extensive alpine glaciation, it has the potential through remote sensing to provide researchers with information about glacier behaviour and hazardous activity.

As two potential areas for further research, high mountain hazards and glacier behaviour are seemingly at odds with each other for remote sensing studies. In local regions (at the glacier scale) where there is a great deal of mass wasting, debris cover creates an often insurmountable obstacle for glacier studies. At the same time, in places where there is regular glacier behaviour in response to climate change, there is little hazardous activity. Fortunately for researchers of both disciplines, the Central Caucasus is a region that provides both.

Many Caucasus glaciers respond regularly to climate change. This study investigates glacier behaviour over the period between 1971 and 1999, which, as it happens, is a relatively stable period of climate fluctuation. Interannual variability of the climate variables temperature and precipitation is high, but does not show any indication of *change* over between 1971 and 1999.

Accordingly, the glaciers of the Central Caucasus have shown some retreat, though not a great amount in relative terms. The retreat exhibited is suggested to have been caused by a climate signal that is not detectable over the period of this study. Glaciers, particularly the larger ones, are probably acting in response to a trend an order of magnitude larger than the observed time-series. However, small glaciers in the region have exhibited lesser amounts of retreat. This could be a direct, short-term response of the stable climate.

The mass balance regime of Djankuat Glacier provides additional useful information about the regional climate. Over the period of this study, Djankuat has had a slightly negative cumulative balance, suggesting that its behaviour in terms of size and shape may reflect that which has occurred to glaciers of this study area. It supports the proposal that a larger climate signal may be responsible for reduction in mass of some of the glaciers in the Central Caucasus. Moreover, in the past seven years since the end of this study, temperatures have shown a stronger warming signal near Djankuat, and the net balance has been increasingly negative.

Rapid melting of glaciated regions associated with climate warming may continue to contribute significantly to sea-level rise in the future. Assessment of this scenario can only be achieved with complete, worldwide knowledge of glacier fluctuations. Although the contribution from small alpine and valley glaciers may be small, they remain a significant source of freshwater, important to the local environment. Their growth and decay in the Caucasus region will continue to have a profound impact on the regional watershed and local communities. For these reasons, glacier research in the Caucasus should be continued and expanded into the future to monitor the retreat of Caucasus mountain glaciers and to evaluate the causes, whether they are climatic or terrain-induced.

REFERENCES

Benn, D. I. and Evans, J.A. 1998. *Glaciers and Glaciation.* John Wiley & Sons. New York, NY

Bronge, L.B. and Bronge, C. 1996. Landsat TM-data and ground radiometer meansurements for snow and ice type classification in the vestfold hills, East Antarctica. *Proceedings of the Fourth Circumpolar Symposium on Remote Sensing of the Polar Environments, Lyngby, Denmark.* European Space Agency SP-391, pp.71-80

Dozier, J. and Marks, D. 1987. Snow mapping and classification from Landsat Themaic Mapper data. Annals of Glaciology. **9**, pp.97-103

Dyurgerov, M. B. and Meier, M. F. 1997. Mass balance of mountain and subpolar glaciers: a new global assessment for 1961-1990. Arctic and Alpine Research. **29**(4), pp. 379-391

Dyurgerov, M. 2002. *Glacier Mass Balance and Regime: Data of Measurements and Analysis*. Occasional Paper No. 55. Institute of Arctic and Alpine Research, Colorado. 88 pp.

Global Land Cover Facility (GLCF). Accessed 25, Feb. 2007. http://glcfapp.umiacs.umd.edu:8080/esdi/index.jsp

Hall, D.K. et. al. 1987. Characterization of snow and ice reflectance zones on glaciers using Landsat Thematic Mapper data. Annals of Glaciology. **9**, pp.104-108

Hall et. al. 1995. Changes of glaciers in Glacier Bay, Alaska, using ground and satellite measurements. Physical Geography. **16**(1), pp.27-41

Hall, M.H.P. and Fagre, D.B. 2003. Modelled climate-induced glacier change in Glacier National Park, 1850-2100. Bioscience **53**(2), pp. 131-140

Harper, J.T. 1993. Glacier terminus fluctuation on Mt. Baker, Washington, U.S.A., 1940 1990, and climatic variations. Arctic and Alpine Research **4**, pp. 332-340

Heybrock, W. 1935. Earthquakes as a cause of glacier avalanches in the Caucasus. Geographical Review. **25**(3), pp. 423-429

Horvath, E., and Field, W.O. 1970. Chapter 3. Glaciers of the Kavkaz (Caucasus) *in* Mountain Glaciers of the Northern Hemisphere. Field, W.O. (ed) 1975. US Army Corps of Engineers, Hanover, New Hampshire, USA. pp. 199-234

Huggel, C. et al. 2006. Modeling and analysis of the 2002 Kolka Glacier erosion, avalanche formation and dynamics, and downstream mudflow hazards. Proceedings of the International Conference on High Mountain Hazard Prevention, Vladikavkaz-Moscow, June 23-26, 2004, Vladikavkaz, 196-203

IASH (ICSI)-UNESCO, 1967: *Fluctuations of Glaciers (FOG) 1959-1965*, Vol. I. Zürich. Compiled for the Permanent Service on the Fluctuations of Glaciers of the IUGG-FAGS/ICSU by Kasser, P. Paris. 52 pp.

IAHS (ICSI)-UNESCO, 1973: *Fluctuations of Glaciers (FOG) 1965-1970*, Vol. II. Zürich. Compiled for the Permanent Service on the Fluctuations of Glaciers of the IUGG-FAGS/ICSU by Kasser, P. Paris. 357 pp.

IAHS (ICSI)-UNESCO, 1977: *Fluctuations of Glaciers (FOG) 1970-1975*, Vol. III. Zürich. Compiled for the Permanent Service on the Fluctuations of Glaciers of the IUGG-FAGS/ICSU by Müller, F. Paris. 269 pp.

IAHS (ICSI)-UNESCO, 1985: *Fluctuations of Glaciers (FOG) 1975-1980*, Vol. IV. Zürich. Compiled for the Permanent Service on the Fluctuations of Glaciers of the IUGG-FAGS/ICSU by Haeberli, W. Paris. 265 pp.

IAHS (ICSI)-UNEP-UNESCO, 1988: *Fluctuations of Glaciers (FOG) 1980-1985,* Vol. V. Zürich. World Glacier Monitoring Service. Compiled by Haeberli, W. and Müller, P. Paris. 290 p.79

IAHS (ICSI)-UNEP-UNESCO, 1993: *Fluctuations of Glaciers (FOG) 1985-1990*, Vol. VI. Zürich. World Glacier Monitoring Service. Compiled by Haeberli, W. and Hoelzle, M. Paris. 322 p.

IAHS (ICSI)-UNEP-UNESCO, 1998: *Fluctuations of Glaciers (FOG) 1990-1995*, Vol. VII. Zürich. World Glacier Monitoring Service. Compiled by Haeberli, W., Hoelzle, M., Suter, S. and Frauenfelder, R. 296 pp.

Kuhn, M. 1984. Mass budget imbalances as criterion for a climatic classification of glaciers. Geografiska Annaler. Series A, Physical Geography. **66**(3), pp. 229-238.

Kuhn, M., 1993: Possible future contributions to sea level change from small glaciers – Chapter 8 *in* R. A. Warrick, E. M. Barrow and T. M. L. Wigley (eds), *Climate and Sea Level Change Observations, Projections and Implications*. Cambridge, Cambridge Univ. Press, pp.134-143.

Oerlemans, J. 2002. Glaciers and Climate Change. A.A. Balkema Publishers. Lisse.

Oerlemans, J. and Fortuin, J. P. F. 1992. Sensitivity of glaciers and small ice caps to greenhouse warming. Science **258**, pp.115-117.

Oerlemans, J.. 1998. Modeling of response of glaciers to climate warming. Climate Dynamics **14**, 267–274

Oerlemans, J. et al. 1998. Modelling of glacier fluctuations. Chapter 5. UNESCO, *in* Haeberli, W., Hoelzle, M., Suter, S. (eds) *Into the Second Century of World Glacier Monitoring - Prospects and Strategies. A contribution to the IHP and the GEMS.* Prepared by the World Glacier Monitoring Service. UNESCO Publishing. pp. 85-96.

Oerlemans, J., Anderson, 1998: Modeling of response of glaciers to climate warming. *Climate Dynamics* 14: 267–274.

Orheim, O. and Luccitta, B.K. 1987. Snow and ice studies by Thematic Mapper and MSS Landsat images. Annals of Glaciology. **9**, pp.109-120

Paul, F. et. al. 2002. The new remote-sensing-derived Swiss glacier inventory I. Methods. Annals of Glaciology. **34**, pp.355-361

Paul et. al. 2003. Glacier monitoring from Landsat TM: problems and perspectives. *EGS - AGU - EUG Joint Assembly.* Abstracts from the meeting held in Nice, France, 6 - 11 April 2003, abstract #4417

Perov, V.F. 1978. Modern exogenous processes in the mountainous territories of the USSR (abstract). Arctic and Alpine Research. **10**(2), pp. 346-346

Meier, M. F. 1984. Contribution of small glaciers to global sea level. Science. **226** (4681), pp. 1418-1421

Meier, M. F., 1965: Glaciers and Climate. In: *The Quaternary of the United States.* (Wright, H. E. and D. G. Frey, eds.), Princeton University Press, pp. 795-805

New, M., Hulme, M., Jones, P. 2000. Representing twentieth-century space-time climate variability. Part II: Development of 1901-96 monthly grids of terrestrial surface climate. pp. 2217-2238

Nitikin, S.A. et al. 2000. Results of radio echo sounding of surging glaciers in the Caucusus and Pamirs. Katalog Lednikov. **99**, pp. 151-153

Schytt, V. 1967. A study of ablation gradient. Geografiska Annaler. **49A**(2-4), pp. 327 - 332

Sidjak, R.W. and Wheate, R.D. 1996. Glacier mapping and inventory of the Illecillewaet River basin, British Columbia, Canada, using Landsat TM and digital elevation data. *Proceedings of the Fourth Circumpolar Symposium on Remote Sensing of the Polar Environments, Lyngby, Denmark.* European Space Agency SP-391, pp.47-51

Townsend, J.R.G. and Justice, C.O. 1988. Selecting the spatial resolution of satellite sensors required for global monitoring of land transformations. International Journal of Remote Sensing. **9**, pp. 187-236

Townsend, J.R.G. and Justice, C.O. 1990. The spatial variation of vegetation changes at very coarse scales. International Journal of Remote Sensing. **11**, pp. 187-236

Townsend, J.R.G. et al 1992. The impact of misregistration on the detection of changes in landcover. IEEE Transactions on Geoscience and Remote Sensing. **30**, pp. 1054-1060

Tucker, C.J., Grant, D.M. and Dykstra, J.D. 2004. NASA's global orthorectified Landsat dataset. Photogrammetric Engineering and Remote Sensing. **70**(3), pp. 313-322

Tutubalina, O.V. et al. 2007. Glacier and debris flow disasters around Mt. Kazbek, Russia/Georgia. 4th DFHM Conference, Chendu, China, 10-13 September 2007.

Waddington, E.D. and Marriott, R.T. 1986. Ice divide migration at Blue Glacier, U.S.A. Annals of Glaciology **8**, pp. 175-176

Warrick R.A. et al. 1995. Changes in sea level. In: Houghton JT, Meira Filho LG, Callander BA, Harris N, Kattenberg A, Maskell K (eds) Climate Change. Cambridge University Press, pp 363-405

Wessels, et. al. 2001. Remotely measuring glacial features using ASTER and Landsat ETM+. American Geophysical Union. Fall Meeting 2001, abstract #IP41A-11

Williams, R.S. and Hall, D.K. 1993. Glaciers. *in Atlas of Satellite Observations Related to Global Change*. Gurney, R.J. Foster, J.L. and Parkinson, C.L. (eds). Cambridge University Press, Cambridge.

World Glacier Monitoring Service (WGMS) website. Accessed 15 Apr. 2007 http://www.geo.unizh.ch/wgms/

Zemp, M. et al. 2005. Worldwide glacier mass balance measurements: general trends and first results of the extraordinary year 2003 in Central Europe. Katalog Lednikov **99**, pp. 3-12